Alluvial fan facies of the Qazvin Plain: paleoclimate and tectonic implications during Quaternary

Azam Davoudi, Saeed Khodabakhsh*, Behrouz Rafiei
Bu-Ali Sina University, Faculty of Sciences, Department of Geology, Hamedan, Iran
**Corresponding author, e–mail: skhodabakhsh@Yahoo.com*
(*received: 14/03/2019 ; accepted: 19/06/2019*)

Abstract
The present study provides a detailed facies description and interpretation of five alluvial fans of the Qazvin Plain. In addition to tectonic activities, which lead to the localization of the alluvial fans on the northern margin of the Qazvin Plain, climate also plays a significant role in the occurrence of facies in these fans. The alluvial fans are divided into three facies groups: group 1 (alluvial fan 1), group 2 (alluvial fans 2, 4, and 5), and group 3 (alluvial fan 3). Alluvial fan 1 is dominated by the episodic matrix to clast-supported gravel (interbedded with a subordinate) and red matrix-supported gravel deposited by non-cohesive debris flow. Groups 2 and 3 are characterized by deposits of non-cohesive debris flow, mud-rich debris flows, channelized, non-cohesive debris flows, hyperconcentrated flows, and sheetfloods. The characteristics of alluvial fan 3 include highly disorganized deposits, very poorly sorted gravel, lack of erosional bases, and a wide particle-size range from clay to outsized-boulders. The facies is best interpreted as a result of debris flow following episodic localized tectonic activities of the Kavendaj Fault along with the fan head during the Quaternary Period. Relatively insignificant changes in the sedimentary facies of the studied fans from debris flows to sheetfloods during the accumulation of the three groups are attributed to a slight variation of climatic conditions, source rocks, and tectonic activities. Therefore, the debris flow-dominated fans of the Qazvin Plain recorded an arid to semi-arid paleoclimate characterized by the generation of non-cohesive debris flow and calcrete in the fans.

Keywords: *Alluvial Fan, Debris Flow, Sheetflood, Paleoclimate, Quaternary Period.*

Introduction

Alluvial fans are among the most important records for tracking climate changes in paleo-environments, hinterland tectonics, and sea/lake levels (Gawthorpe & Leeder, 2000; Bose *et al*., 2012; Chen *et al*., 2016). Climate, tectonic, and hinterland lithology highly affect the grain size and volume of sediments transported into the alluvial fans (Chakraborty & Paul, 2013). Studying these controls on alluvial fan facies without considering their effects is a difficult task to accomplish (Nichols & Thompson, 2005). In this regard, the classification of alluvial fans by Blair & McPherson's (1994) based on combining the involved processes reinforces the traditional hypothesis of 'dry fans and wet fans' (Schumm, 1977) associated with arid and humid climates, respectively. However, the validity of climate-response hypothesis remains still in debate (i.e., Harvey *et al*., 2005; Blair & McPherson, 2009; Harvey, 2012). In addition, previous literature has revealed that a more humic climate leads to a larger number of flood events and also more mud fraction, as a result of the increased vegetation and chemical weathering (Blum & Tornqvist, 2000). Under this humid condition, debris-flow activity on the fans is intensified whereas climatic aridification increases the fluvial activity on fans (Chen *et al*., 2016). Moreover, climatic changes control the nature of fan deposits under arid or semi-arid conditions (Frostick & Reid, 1989). Fine sediments are deposited under warmer and drier conditions, whereas high flood discharge and sediment under wet and cool conditions lead to a high deposition rate of coarse sediments (Koltermann & Gorelick, 1992). The main objective of this study is to investigate the Quaternary alluvial fans in the NE margin of the Qazvin Plain. In the study area, the uplift and the climatic fluctuation during the Quaternary had profound control on geomorphic, sedimentary, and pedogenic processes. In this paper, primary depositional processes and secondary (in situ) carbonate deposition in modern alluvial fans are discussed. The results are therefore applicable for other fans deposited in similar settings. To the best of our knowledge, no previous research has been conducted on sedimentological and paleoenvironmental characteristics of these fans. Overall, the purposes of this study are 1) to describe and interpret the sedimentary facies and internal structures of the Quaternary deposits of alluvial fan systems and 2) to discuss the role of climate, tectonics, and lithology on the sedimentary facies.

Geological setting

Iran is located in the middle part of the active

Alpine-Himalayan orogenic belt. This country has been deformed due to the convergence of the Arabian plate to South Asia (Allen *et al*., 2003; Copley & Jackson, 2006). The Qazvin Plain, located adjacent to the Central Alborz Range in northern Iran, is a structural plain (graben) formed because of the activity of the north Qazvin and Ipak faults. This plain is filled by aggradation of various sedimentary processes such as alluvial fans, fluvial systems, playas, and aeolian deposits (Berberian *et al*., 1993). Rieben (1966) classified the alluvial sediments of the Qazvin Plain margins into four lithological units: Alluvial A, B, C, and D (from base to top, in the order of their appearance). The sediments of this plain are mainly composed of conglomerates, sandstones, and mudstones with local evaporate and calcrete deposits (mainly occurred as powdery, chalky, nodular, massive, and laminar). The sediments thickness of the central part of the plain is up to 350 m (Berberian *et al*., 1993); however, there is limited geophysical data about the plain basement depth. The only evidence on the plain basement is the outcrop of the Karaj Formation (Eocene) in the north and south of the Qazvin area (Berberian *et al*., 1993). This formation is comprised of a relatively thick sequence of well-stratified green tuffs, sedimentary rocks, and volcanic lava and rare evaporative rocks (Annells *et al*., 1975). Most alluvial fans of the region are located along the northern margin of the Qazvin Plain (Fig. 1). They occur adjacent to the compressive faults of the north Qazvin, two of which (i.e., the Qazvin North and Kavendaj faults) being recently seismically active (Berberian *et al*., 1993). Based on their dominant catchment lithology, these fans may be divided into two groups: 1) well-stratified carbonate rocks and fine-grained clastic sediments (mainly mudstone and siltstone) and 2) volcaniclastic rocks (i.e., green tuff) associated with other clastic sedimentary rocks (e.g., conglomerate, sandstone, and mudstone) (Annells *et al*., 1975). The first group is seen in the Fan 1 catchment and the latter mainly makes up catchment of the other fans. The study area has an arid to a semi-arid climate with an average annual temperature of 12 to 14℃ and annual precipitation of 220 mm (Meteorological Organization of Iran, 2011).

Material and Methods

Five alluvial fans existing along 42.56 km north of the plain were studied (Fig. 1).

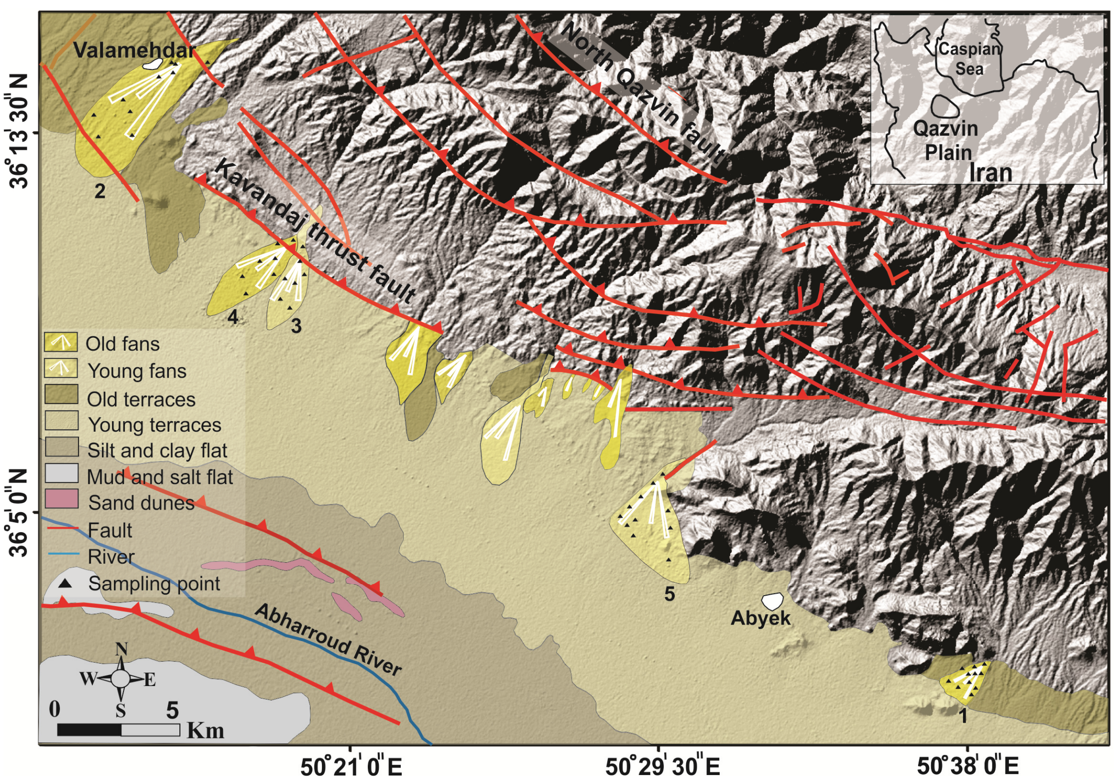

Figure1. Location map of the studied alluvial fans (1 to 5)

The characteristics of representative profiles including sedimentary structures, texture, bed geometries, and lithology were used to describe fan facies. In addition, paleocurrent directions were depicted using azimuth measurements of imbricated pebbles. Facies were described following Miall's (2006) code system. For this purpose, a total of 355 measurements were used for the reconstruction of paleocurrent directions. Maximum clast size (No. 251) and composition were investigated to obtain information about paleocurrent directions and sediment provenance, respectively. Mineralogical composition of representative bulk and oriented samples was investigated by X-ray diffraction (XRD) in Bu-Ali Sina University, Iran (Italstructures, 40 Kv, Cukα 30mA). Also, scanning electron microscopy (SEM) was performed on the representative samples at the Bimgoster Laboratory, Iran (Mira3-TESKAN Scanning Electron Microscope, 20KV). Moreover, X-ray fluorescence analysis (XRF) of 10 non-calcareous samples (Table 1) was carried out to assess CIA (Chemical Index of Alteration; Nesbitt & Young, 1982) and CIW (Chemical Index of Weathering; Harnois, 1988).

Facies characteristics

Gravelly facies in this study area made up of more than 85% of the studied profiles. In some horizons, they are slightly consolidated and therefore may be considered as conglomerates. Sand and mud are subordinate facies. Generally, a distinct downward fining trend (toward the fan toe) is observed. All the studied sediments are red. Their common characteristics are basal non-erosional surfaces, mud cracks, and local/discontinuous calcrete horizons. A total of 8 gravel/conglomerate lithofacies, a sand lithofacies, and 3 types of calcrete facies were identified (Table 2).

Facies characteristics

Gravelly facies in this study area made up of more than 85% of the studied profiles. In some horizons, they are slightly consolidated and therefore may be considered as conglomerates. Sand and mud are subordinate facies. Generally, a distinct downward fining trend (toward the fan toe) is observed. All the studied sediments are red. Their common characteristics are basal non-erosional surfaces, mud cracks, and local/discontinuous calcrete horizons. A total of 8 gravel/conglomerate lithofacies, a sand lithofacies, and 3 types of calcrete facies were identified (Table 2).

Facies A: Massive to crudely stratified matrix-supported gravel (Gmm)

This facies consists of matrix-supported gravel. It displays planner beds with a thickness of a few decimeters to ∼4 m. The beds are locally stratified and their lateral continuity varies from a few meters to tens of meters along profiles (Fig. 2).

Table 1. Data values of elemental composition of ten samples from five alluvial fans studied in this research. Mf is the abbreviation of mudflow.

Sample no.	SiO_2 (%)	Al_2O_3 (%)	Fe_2O_3 (%)	TiO_2 (%)	CaO (%)	MgO (%)	Na_2O (%)	K_2O (%)	P_2O_5 (%)	MnO (%)	LOI (%)	BaO (%)	SrO (%)	CIA	CIW
F1 -1	47.30	6.91	2.91	0.36	9.27	3.16	0.33	1.09	0.11	0.09	28.28	0.12	0.05	39.27	41.85
F1 -2 (mf)	55.50	8.42	5.83	0.59	6.08	2.89	0.63	1.99	0.16	0.15	20.96	0.04	0.05	49.16	55.63
F1 -3	45.52	6.58	3.81	0.23	5.86	7.16	0.98	1.37	0.09	0.18	27.98	0.19	0.05	44.48	49.03
F2 -1	45.47	13.59	6.26	0.63	10.79	2.28	1.16	1.90	0.26	0.08	17.42	0.10	0.06	49.53	53.21
F4 -1	47.39	6.92	3.87	0.36	9.45	1.64	0.62	1.09	0.27	0.07	28.19	0.06	0.05	38.29	40.74
F4 -2	58.96	15.15	3.53	0.68	6.73	1.32	1.50	1.25	0.53	0.08	10.16	0.04	0.06	61.51	64.80
F5 -1	32.40	11.81	11.77	0.66	7.31	5.57	2.61	1.19	1.43	0.06	25.08	0.04	0.05	51.53	54.35
F3 -1	39.38	8.92	5.81	0.35	8.47	5.88	0.59	2.08	0.14	0.07	28.18	0.06	0.05	44.48	49.62
F3 -2	52.28	6.83	3.87	0.31	7.37	2.24	0.65	1.08	0.12	0.11	24.98	0.10	0.04	42.89	46.00
F3 -3	50.21	9.97	5.85	1.38	8.65	1.64	0.62	1.12	0.15	0.09	20.19	0.06	0.05	49.03	51.88

Table 2. Facies of the alluvial fans of The Qazvin Plain.

Facies	**Sedimentary structures**	**Bed geometry and thickness**	**Depositional process**	**The occurrence in alluvial fans**
A. Massive to crudely stratified; matrix- to clast-supported gravel (Gmm)	Poorly sorted, matrix- to clast-supported, clast alignment, vague imbrication. Massive to crudely stratified. Lack of cross-stratification and erosional bases. Outsized clasts (Fig. 2).	Tabular; 90-400 cm	It was deposited by non-cohesive debris flow (Schultz, 1984; Miall 2006; Blair & McPherson, 2009).	All fans
B: Matrix-supported disorganized bouldery gravel (Gmm)	Very poorly sorted and disorganized, matrix-supported. Abundant outsized sub-angular to sub-rounded clasts. Absence of erosive bases (Fig. 3).	Tabular to wedge-shaped; 60-170 cm	Deposits of sediment-gravity flow resulting from flash flood events or rock avalanche (Blair, 1999; Moscarielo 2017) following episodic tectonic activity such as the fault reactivation.	Fan 3
C. Rhythmic gravelly and sandy planar couplets (Gcm and Gmm/Sm)	Matrix- to clast-supported couplets dominantly from rhythmically cobbly pebble gravel interbedded with pebbly sand and/or matrix supported gravel. With the same thickness and textures. Coarse clasts are generally oriented parallel to sub-parallel to the bed surface. Non-erosive and sharp contact between alternating beds. Occasionally associated with backset-beds (or antidune cross-bedding), HCS-like or HCS-mimics and normal grading structures (Fig. 4).	Tabular; 70-260 cm	Deposits of sediment-charged upper flow regime resulting from rapid drainage of a large volume of water from the catchment after heavy rainfall (Mutti et al., 1996; Galloway *et al.,* 1996; Blair 1999).	All fans
D. Graded clast-supported gravel (Gmg)	Poorly to moderately sorted, clast- to matrix-supported, and sub-angular clasts, erosional basal surface and a floor of coarse imbricated clasts. Clast imbrication. Normal grading (Figs. 4a and d).	Lenticular to channel-shaped; 50-200 cm	Channel infilling by lags and bars (Miall, 2006).	All fans
E. Crudely, planar, cross-bedded cobbly pebble gravel (Gp)	Poorly sorted, matrix- supported, crudely fining-upwards, planar cross-bedding. Erosional to non-erosional bases (Fig. 5).	Tabular to lenticular; 140-150 cm	Deposits of a) foreset cycles as a result of the downstream migration of bedforms typical of mid-channel or longitudinal bars (Nemec & Postma 1982; Ghinassi & Ielpi, 2016), b) hyperconcentrated flashy streams in braided channels, or C) vertically stacked debris flows (Miall, 2006).	
F. Massive to crudely stratified clast-supported gravel (Gcm)	F1. Poorly to moderately sorted and clast-supported. Sharp and non-erosional bases. Ungraded or crudely stratified and inverse grading (Figs. 6a and b). F2. Poorly sorted and clast-supported. Well imbricated, sub-angular to sub-rounded clasts. Inverse grading. Wide range of clast size (Figs. 6c and d). F3. Concentrated pebbles. Clast-supported and well sorted. Sharp bases. Ungraded to local coarse tail. Bimodal texture (Figs. 6e and f).	Tabular to wedge-shaped; 50-250 cm Lenticular; Up to 150 cm Lenticular; 110 cm	Deposition of pseudoplastic cohesionless debris flow (or turbulent flow) (Miall, 2006). Channelized hyperconcentrated flow (Miall, 2006). Sieve deposits as a result of removal of fine sediments from the coarse fraction by sheetflood or overland flow winnowing (Hooke, 1967; Bull, 1972; Blair, 1999a; Blair & McPherson, 2009)	All fans
G. Trough cross-bedded gravel (Gt)	Poorly sorted, well organized, matrix- to clast- supported, trough cross-bedding. Ungraded or normal grading. Erosional basal contact (Figs. 7a and b).	Lenticular to channel–shaped; 30-70 cm	Deposits of migrating bedforms within scours and/or channels formed at high flood-stage (Miall 2006).	Fan 5
H. Structureless muddy (pebbly) sandstone (Sm)	Moderately sorted medium to coarse gravelly sands with dispersed granules and pebbles, internally massive. Non-erosive basal contact with local scouring (Fig. 7c).	Tabular; 20-220 cm	Deposits of sediment-gravity flow within the distal areas of the alluvial fans (Miall, 2006).	All fans
I. Calcrete (P)	Authigenic carbonate, with various macro- and micro-morphology features (Figs. 8 and 9).	Powdery to massive; 50-200 cm	Secondary carbonate accumulation	Fan 1, 2 and 5

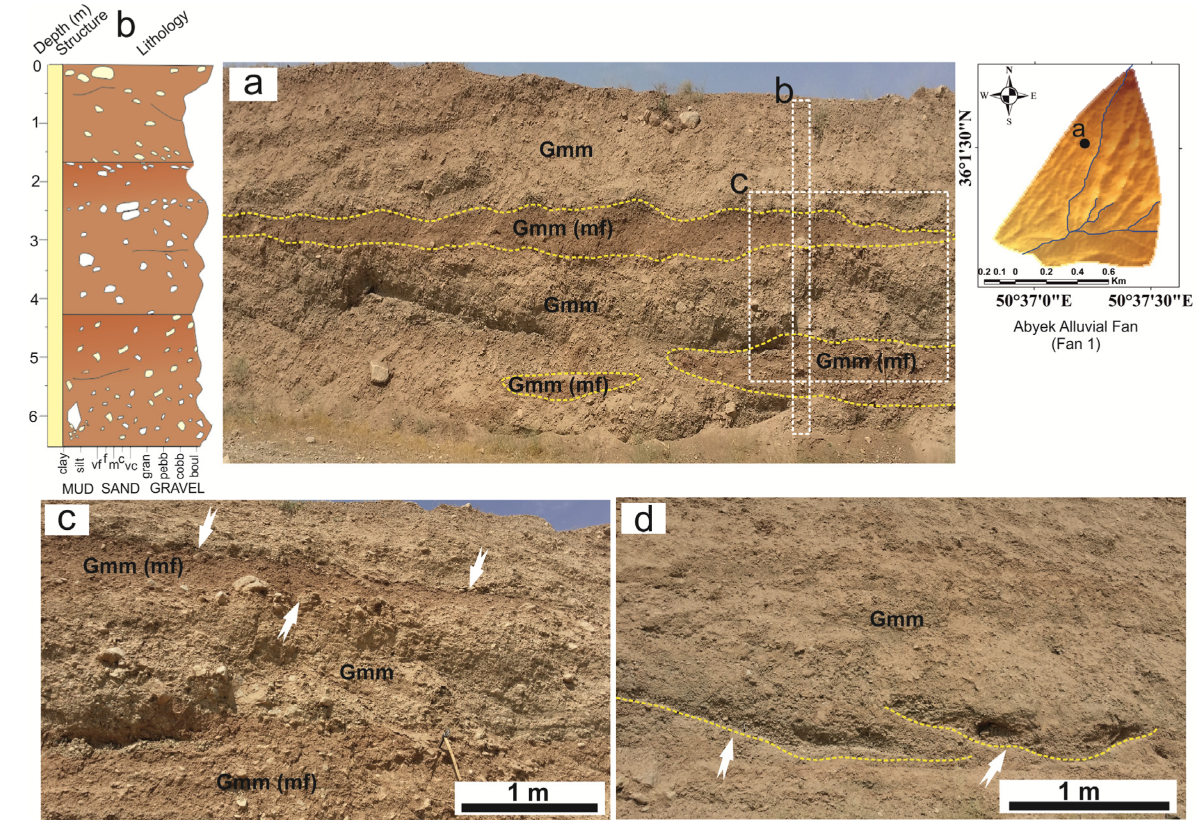

Figure 2. Sediment profile and photographs of facies A. a-b) matrix- to clast-supported gravel (Gmm) and interbedded, lenticular, red-colored, matrix-supported gravels or mudflows (mf). c) Close-up photos of Gmm and mf facies. d) Lenticular, cobble-gravel channel bodies. The inset map shows the location of the profile in the fan surface.

It is poorly sorted and the clasts are pebble to boulder size. It exhibits crude imbrication, clast alignment, floating outsized the clasts or protruded above the bed tops. Few erosional bases may be present. The beds are sub-parallel to parallel to the fan surface. Marked changes in color, matrix content, clast-grain size distribution, and the bed contacts are observed in some beds. They are up to 1 m thick and the fine fraction of their matrix is up to 50% (i.e., mudflows in Figs. 2a and 2c). These interbeds have a marked gradual contact with the lower coarser beds; however, their upper contact is sharp. Angular to subrounded clasts in interbeds are cobble-sized to local boulders up to 20 cm in diameter. In addition, poorly developed, thin layers of pebbles and coarse cobbles (commonly one clast thick) above and below mudflow lenses are observed (Fig. 2c). Moreover, in proximal parts, lens-shaped cobble-filled channel bodies occur in the facies (Fig. 2d). The channel width and depth are few meters to less than 0.5 m, respectively. The channel-fill sediments are structureless or show crude normal grading.

Interpretation

The facies exhibit typical features of debris flow deposits (Bull, 1972; Nemec & Steel, 1984; Schultz, 1984, Blair, 1999b; Blair & McPherson, 2009) characterized by episodic deposition (Mather, 2016). The prominent matrix-supported character and random orientation of clasts indicate the matrix buoyancy as the dominant transportation and depositional processes in which clasts were unable to move freely (Walker, 1975). During such flows, the outsized boulders are supported by the mechanical strength of the matrix due to a high sediment concentration of fluid (Rodine & Johnson, 1976). Moreover, the rare erosive bases, vague imbrication, and clast alignment are indicators of laminar flow with shear strength caused by low water concentration and high matrix strength rather than normal traction currents (Sohn et al., 1999). Local stratified clasts in this facies are formed as a result of clast-alignment parallel to their long axes (Turkmen *et al.*, 2007). In addition, the gradational base of the mud-rich flows that overlie the debris-flow deposits proposes a possible link between the two depositional processes. The former is interpreted as a waning (dilute) cap of the underlying debris flow (Went, 2005). This cap forms in the final depositional stages of debris flows, in which a watery mud with scarce clasts develops (Blair & MacPherson, 1998). Losing boulders by getting farther from the apex of the alluvial fan causes boulder-deficient center and lower parts of the debris flow to continue downslope, where it is accumulated as a clast-rich lobe. Then, a clast-poor lobe stage occurs as a result of the more dilute tail of debris flow, capping the downslope ends of the clast-rich lobes on the low-gradient distal domain (Blair & McPherson, 2009). The red color of this facies reflects subaerial oxidation condition (Walker, 1967). Poorly developed thin pebbly layers are formed as weakly defined armors above and below mud lenses (Lindsey *et al.*, 2005).

The cobble-rich lenses with an erosive base are formed through the winnowing, scouring, and armoring the host deposits by local runoff events (Blair & McPherson, 1998; Blair, 1999a), giving rise to local lag concentration. Their limited thickness is due to the low power of surface runoffs and also the self-limiting nature of the armoring process (e.g., Parker & Sutherland, 1990; Kleinhans & van Rijn, 2002; De Haas *et al.*, 2014). The discontinuity of this lens-shape deposit within and/or on debris-flow beds is as a result of the spatially fractionated distribution of surface runoffs over the fan surface (De Haas *et al.*, 2014) and highly variable discharge near the mountain front (Lindsey *et al.*, 2014).

Facies B: Matrix supported disorganized bouldery gravel (Gmm)

The main characteristics of this facies are abundant outsized boulders, variability in size and composition, a very poorly sorted matrix (ranging from clay to pebbles), and a non-erosive base (Fig. 3). The maximum clast size range is from 0.3 to 1.3 m (Av= 0.45 cm). The geometry of the layers is tabular - to wedge-like. This facies occurs only in fan 3 and constitutes 40% of its area. This facies is alternated with wedge-shape clast-supported gravels. The latter facies has eroded the lower matrix-supported facies (Fig. 3a), and all parts of the fan surface (from apex to toe) are covered by a mantle of boulders (Figs. 3c and d).

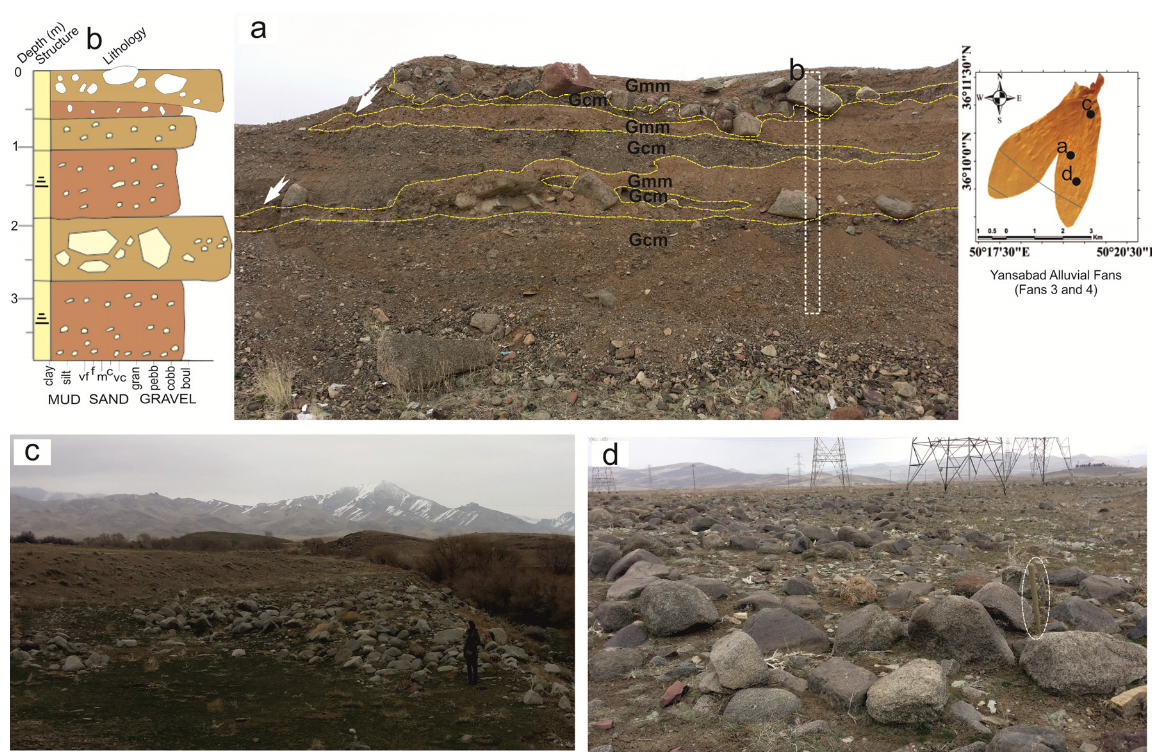

Figure 3. Sediment profile and photographs of facies B. a-b) matrix-supported, disorganized, unsorted gravel composed of cobbles to outsized boulders (Gmm), which is interbedded with the crudely stratified clast-supported (Gcm). Note wedging out of the Gmm facies in the up-current direction (with arrow). C-d) boulder mantle on the surface of the fan. The scale (hammer) length= 45 cm (d). The inset map shows the location of the profile in the fan surface.

They display a very poorly sorted massive fabric with local coarse tail inverse grading, vague imbrication, and clast alignment.

Interpretation

Sedimentary features of this facies include very large outsized clast, very poor sorting, sheet- to wedge-like bed geometry, the polymictic composition of clasts, non-erosional bases, local inverse grading, clast alignment, and the lack of cross-bedding. They are often typical of sediment-laden debris flows resulting from flash flood events and/or from rapid waning flows that do not allow reworking and effective sorting of surface deposits (Blair, 1999a; Moscarielo, 2017). This facies occurs only in fan 3, where the Kavendaj Fault has cut the upstream margin of the fan. Some boulders were directly derived from the catchment area, transported and re-deposited by flash floods. Moreover, tabular - to wedge-shaped geometry and alternating with wedge-shaped facies Gcm may suggest that episodic reactivation of the Kavendaj Fault probably played a significant role in the supply of the coarse-grained material to the fan area. The high amounts of the matrix that infiltrated the boulders and cobbles were probably derived from the disintegration of clasts during transportation.

Facies C: Rhythmic planar gravelly and sandy couplets (Gcm and Gmm/Sm)

This facies comprises alternating clast- to matrix-supported gravels. The former consists of cobbly pebble gravel and the latter beds are pebbly sand and/or matrix supported gravel (Fig. 4a). This horizontal to sub-horizontal couplets are common in the alluvial fans 2, 3, 4, and 5. Coarse clasts tend to be sub-angular to angular, poorly to moderately sorted, and generally oriented parallel to subparallel to the bed surface. The contact between alternating beds is often non-erosive and sharp. The field evidence shows that these couplets are associated with a set of diagnostic features such as occasional backset-beds (or antidune cross-bedding) (Fig. 4c), HCS-like or HCS-mimics (Figs. 4e and f) (Rust & Gibling, 1990; Masuda *et al*., 1993), and normal grading. This set is volumetrically subordinate and is mostly absent in the successions of alluvial fans (Moscarielo, 2017). Cross-lamination in the vertical profile (Fig. 4c), i.e., dipping both upstream and downstream, is a distinct characteristic of the antidune deposits. Antidune cross laminae are relatively low-dip angles and vague and therefore can be detected easily (e.g. Middleton, 1965; Barwis & Hayes, 1985). We found HCS-like sedimentary structures near the top of a 3.9-m-thick sheetflood conglomerate. This unit is characterized by wavy laminae. The bedform wavelengths were 45-120 cm and the amplitudes ranged from 15 to 35 cm. Antidune bedforms have mainly been formed in a wide range of grain sizes from cobble to very fine sand or silt and are graded vertically and laterally into flat, planar laminations.

Interpretation

The rhythmic stacking of the regular couplets arises from the upper-flow regime of supercritical water flow, which is characteristic of sheetflood facies in subaerial conditions (Mutti *et al*., 1996). Sheetfloods are caused by torrential rainfall directly on the surface of the alluvial fan (Galloway et al., 1996). The high volume of water caused by the heavy rainfalls from the catchment area may lead to fluid -gravity flows and sediment transfer through flash floods from the catchment slopes onto the fan. Therefore, the deposition from such sheetfloods is triggered by the migration and washout of the upper flow regime antidune bedforms beneath trains of standing waves on the fan surface (Alenander & Fielding, 1997; Blair, 1999a). The coarse-grained member of a couplet is deposited during the downslope washout phase of standing wave destruction, in which local high turbulence give rise to the suspension of finer sediments. The fine suspended sediment, following a rapid abatement of turbulence, will then deposit on the coarse couplet laminae with a sharp non-erosional contact (Blair, 2001). This alternation in modern fans is considered as bedload followed by the intermittent suspended load from an intense washout (Blair, 1999a). Alternating bed couplets can be due to debris flows and/or sheetfloods in the distal domain of the fan (Amajor, 1986). Other multi-story sheetflood products such as antidune and wavy laminae are also related to supercritical flow with the auto-cyclic nature of standing waves (or trains of water and sediment waves) (Blair & McPherson, 2009). These waves repeatedly 1) initiate, 2) grow up, 3) migrate upslope, and 4) terminate either by gently re-joining the flood or by 5) breaking and shooting downslope. Backset-beds (Middleton, 1965) structures are developed during the first three of these stages. These units are preserved if the standing wave gently combines with the flow (Blair

& McPherson, 2009). Antidune could be used for recognizing the paleocurrent direction, velocities (Middleton, 1965), and high-energy deposits (Slootman *et al*., 2018) in the geological record. The hummocky cross-stratification (HCS)-like structure is a form of antidune stratification that is caused by maintenance of a stationary state of sheetflood standing waves (Hwang *et al*., 2016) along with the interface an overlying low-density layer and a denser underflow in upper flow regime (Araya & Masuda, 2001).

Facies D: Channelized graded clast- to matrix-supported gravel (Gmg)

This facies consists of channel-shaped depositional units (up to 2 m thick and 12 m wide). The typical characters of this facies are monomictic to polymictic clasts, distinct normal grading, moderately to well sorted, clast-supported gravel, and a floor of coarse imbricated clasts (Figs. 4d and 5a).

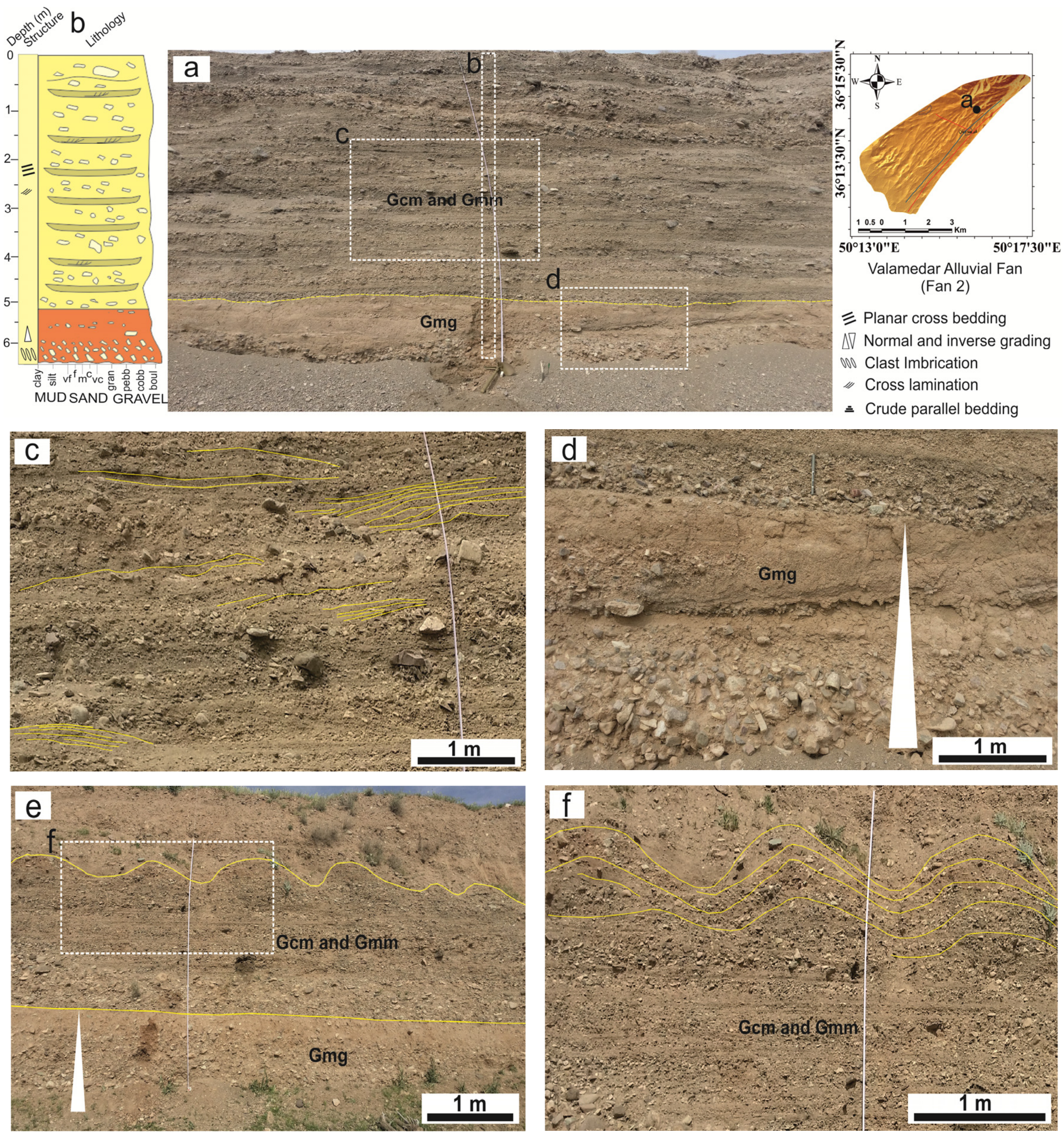

Figure 4. Sediment profile and photographs of facies C and D. a-b) Rhythmic gravelly and sandy planar couplets (Gcm and Gmm) overlying Gmg facies. c) Close-up view of couplets and cross laminations (antidune), dipping both upstream and downstream. d) Close-up view of Gmg facies. e) General view of the sheetflood couplets with HCS-like structures (wavy laminae) and Gmg facies. f) Close-up photos of wavy laminae.

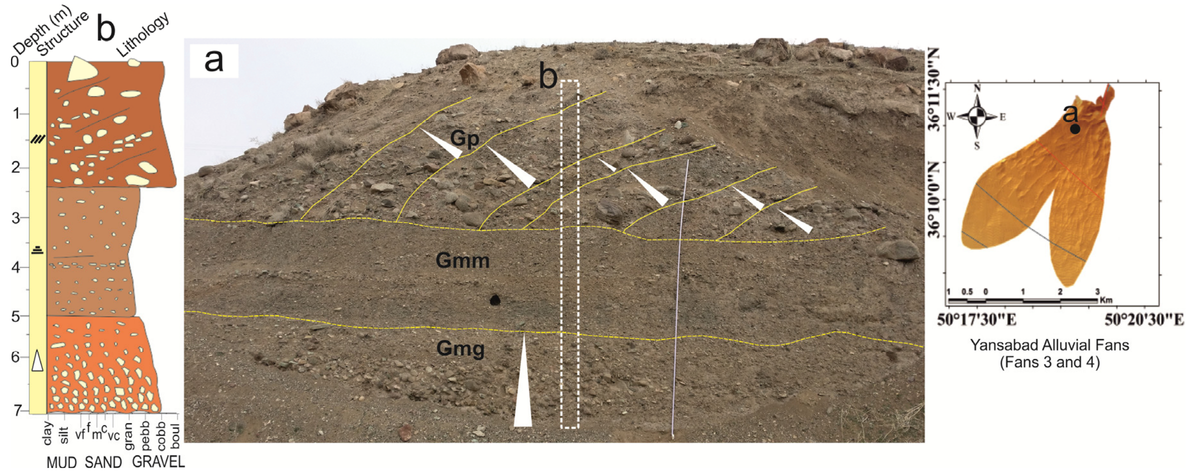

Figure 5. Photo of facies E. a-b) crudely, planar, cross-bedded cobbly pebble gravels overlying Gmm and Gmg facies.

The upper boundary of the conglomerate units is sharp, which is commonly marked by a sudden transition into overlying facies. In some horizons, drapes of finer sediments occur on a coarser base.

Interpretation

Multi-story lensoid to channel-shaped facies are interpreted as incised-channel deposits (scour lags and bars) of the alluvial fan systems, as testified by their geometry and by the erosional nature of their base. Incised channels primarily form as discharge conduits across the fan. Therefore, their sediments mainly consist of an armored channel bed that lies directly on other primary sediments such as debris flows and sheetfloods (Blair & McPherson, 2009). In shallower conditions, muddy deposits on top of channel-fill deposits may be deposited as a consequence of fall-out from waning flow after channel abandonment and avulsion episodes (Bluck, 1980).

Facies E: Crudely, planar, cross-bedded cobbly-pebble gravel (Gp)

This facies appears to be found only in fan 4 and oriented transverse to the southeast direction of stream flow (Fig. 5a). These facies are also subordinate among the facies. The cross-beds are planar with decimeter-thick, and dip angles of them vary from 35 to 45°. In addition, the facies shows crudely fining-upward grading cobbles into medium-grained sandy gravel, sub-angular to sub-rounded clasts, and a non-erosional basal contact scoured in places. The northeastward-dipping imbricated clasts are commonly observed in this facies.

Interpretation

Traction current in this facies is well evidenced through the occasional presence of imbricated clasts and the crude stratification and the crude upward grading. Upward-fining inclined strata may be represented in the following forms: a) foreset cycles as a result of the downstream migration of bar forms typical of mid-channel or longitudinal bars (Nemec & Postma, 1982; Ghinassi & Ielpi, 2016), b) hyperconcentrated flashy streams in braided channels, and c) vertically stacked debris flows (Miall, 2006). Upward-fining grading is proposed to form during channel abandonment or the waning flood stages (Ghinassi & Ielpi, 2016).

Facies F: Clast-supported gravel (Gcm)

This facies can be subdivided into three subfacies F1, F2, and F3. Evidence of facies F1 includes polymict clasts, poor sorting, massive to crudely stratified, clast-supported, subangular to subrounded clasts, moderately to well-developed imbricated, non-erosional bases (erosional in places), the predominant sheet-like geometry, non-graded, and occasionally crudely inverse grading (Figs. 6a and 6b and 3a). The thickness of the beds rarely exceeds 5 m and commonly varies from 1 to 3 m. In alluvial fan 5, this facies is often interbedded with thin clast-poor lobes (< 50 cm).

Facies F2 is well exposed in two 1.2 to 1.5-m-thick sections of fan 2 (Figs. 6c and d), where lensoid conglomerates with poor sorted, clast-supported, and inverse grading are evident. The clasts are well-imbricated, subangular to subrounded, and infilled by coarse sand to the fine pebbly matrix.

Facies F3 consists of a local concentration (thickness=1.1 m and width=4 m) of cobbles and pebbles. This facies has occurred in a sidewall exposure along a mid-fan channel as lag deposits. It is typically lenticular, massive with local coarse tail, clast-supported, and moderately to well sorted, with its base contact marked by winnowed gravels (Figs. 6e and 6f). This facies exhibits a bimodal grain-size distribution. The coarse clasts are mostly sub-rounded to rounded clasts and in some cases are subangular. Bladed pebbles show imbrication.

Interpretation

Sheet-like geometry, clast-supported texture, the presence of boulder-sized clasts on conglomerates with crudely inverse grading (Steel & Nemec, 1982; Postma; 1984), coarse sandy matrix (mud <5%), and non-erosional base (Saula *et al.*, 2002) support origin of facies F1 as product of pseudoplastic cohesionless debris flow (turbulent flow).

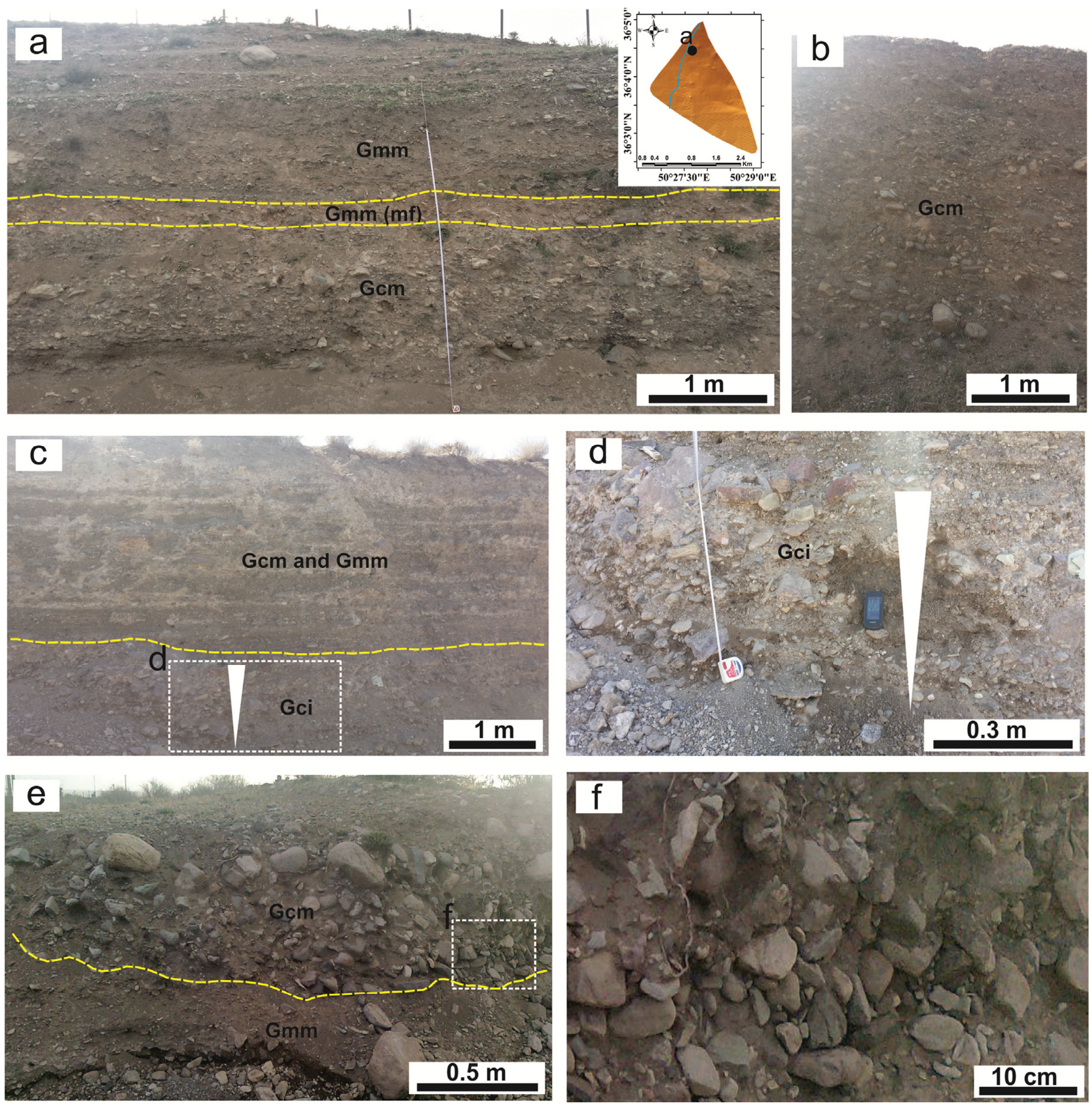

Figure 6. Sediment profile and photographs of facies F. a) facies F1 consists of clast-supported gravels (Gcm) is overlaid by mudflow and Gmm facies. b) facies F1 consists of clast-supported gravels (Gcm). c) facies F2 with inverse grading. d) Close-up view of facies F2. e) facies F3 consists of concentrated clast-supported gravels on the gullied surfaces with bimodal texture and sand to pebble matrix. f) Close-up view of facies F3.

Moreover, ungraded units of mass flow gravels with a-axes imbricated clasts bear definite signatures of operation of dispersive pressure and internal shear of flow (Sarkar *et al*., 2008). Some grain-supported beds contain abundant imbricated fragments, indicating that in most cases deposition is due to unconfined energetic floods (Sanchez-Nunez *et al*., 2014), with high sediment concentration (*sensu* hyperconcentrated flow; Saula *et al*., 2002), which prevents the deposition of fine-grained sediments. Moreover, due to their formation in turbulent conditions, they exhibit a massive texture (Kastic *et al*., 2005). On the other hand, lensoid-shaped deep scours, poor sorting, inverse grading, imbrication, and a wide range of clast size may suggest that facies F2 has been generated by channelized hyperconcentrated flow (Miall, 2006).

Facies F3 with a better sorting compared to other gravelly facies reveals its selective transport and deposition, producing concentrated gravels. It is developed by the winnowing of fine fraction from coarse fractions by sheetflows or overland flows, leaving behind coarse sediments as channelized fills (Blair, 1999b). This facies is called sieve deposits (Bull, 1972).

Facies G: Trough cross-bedded gravel (Gt)
Well-developed trough cross-bedded facies is also found as a minor facies in the alluvial fan 5 (Fig. 7a). This unit is composed of relatively thin cross-bedded/normal graded pebbly sandy gravel (Fig. 7b). They fill scoop-shaped scours and channels with 20-35 cm depths. The foreset dips mainly vary from 20° to 25°, but values up to 30° occur in some troughs.

Interpretation
Occasional trough cross-stratified sets within gravelly units may suggest the low-energy regime during the depositional of coarse-grained units. They are interpreted as having formed by dunes migrating over bars (Harms & Fahnestock, 1965). Some examples of this facies display filling of minor channels (Miall, 2006). Laterally discontinuous trough units within gravelly facies are the deposits of migrating bedforms within scours and/or channels formed at high flood-stage (Martini, 1977; Rust, 1984). Moreover, this case can be formed either by local vortices around the obstacles or by leaving an abandoned channel and channel system avulsion (Miall, 2006).

Facies H: Massive muddy/pebbly sand (Sm)
The layers of this facies are 0.5 to 2 m thick and contain less than 10% randomly scattered pebbles (Fig. 7c), with a non-erosive basal contact.

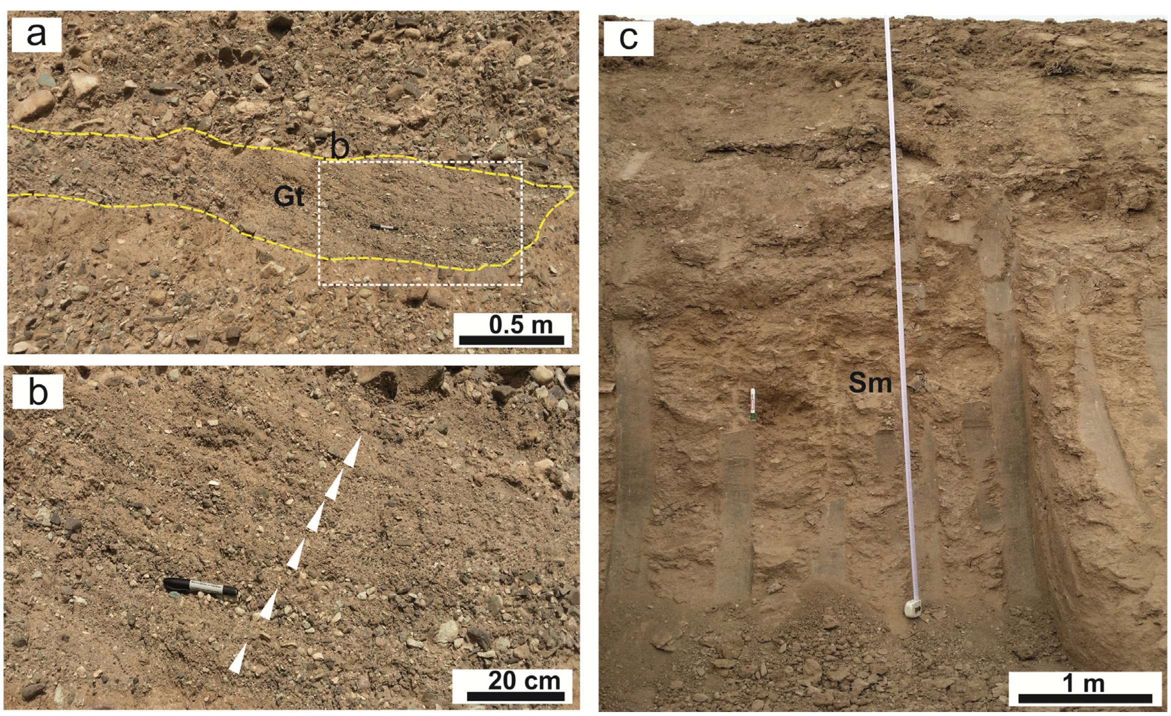

Figure 7. Sediment profile and photographs of facies G and H. a) trough cross-bedded gravels (Gt) infilling scoop-shaped scours. b) Close-up view of facies G. Note amalgamated normal grading. c) facies H consists of massive muddy (pebbly) sandstone (Sm).

In some cases, these layers are rich in abundant small irregularly shaped carbonate patches. This facies typically occurs in the distal domains of the fans.

Interpretation

Overall, the sedimentary fabrics of this facies suggest that they were deposited by sediment-gravity flow within the toe of the alluvial fans (Miall, 2006).

Facies I: Calcrete facies

Calcrete (caliche or authigenic carbonate) occurs in some of the alluvial fans, typically in the alluvial fans 1, 2, and 5. The calcrete profiles of these fans show various macro- and micro-morphology features. These profiles are described individually in the following:

I.1) In the proximal part of fan 1, calcrete horizon occurs as a massive appearance (Fig. 8a). The coated grains, desiccation cracks, and root traces can be seen dominantly in this profile. Petrographically, the massive horizon mainly consists of microsparite groundmass with biogenic microfabrics such as bioturbation, root voids (Fig. 8b), clotted micrite, scattered various cracks filled with calcite cement, and expansion grains as a result of replacement and displacement (Fig. 8c). Moreover, the occurrence of overgrowth of the needle palygorskite on secondary carbonates and detrital grains are common in the calcrete (Fig. 8d).

I.2) In the distal part of fan 2, a powdery and nodular calcrete horizon is observed. This horizon is covered with several non-calcareous alluvial sediment bodies (Fig. 9a). Most remarkable features of secondary carbonate include millimeter-sized whitish powder, coated grains and bands (or thin layers) consisting of diffuse-margin nodules, which mimic the concave-up geometry of channel deposits and/or conform to the stratal planes of the sediment body (Fig. 9b), and disc-shaped (Fig. 9c) and elliptical cream color nodules (Fig. 9d). Other features of this horizon are mottling (or reddish-brown patches) (Fig. 9e) and rhizocretions that occur in different parts of this horizon. Through the petrographic study conducted in this work, the nodules showed dense microsparitic and micritic groundmass accompanied with microfabrics such as bioclasts alveolar septal structures, dendritic Mn-oxide mottlings (Fig. 9f), fenestral porosity (Fig. 9g), clotted micrite, hair-like roots or filaments (Fig. 9h), bacterial organisms (Fig. 9i), biomineralization, microborings or root trace, and palygorskite fibers.

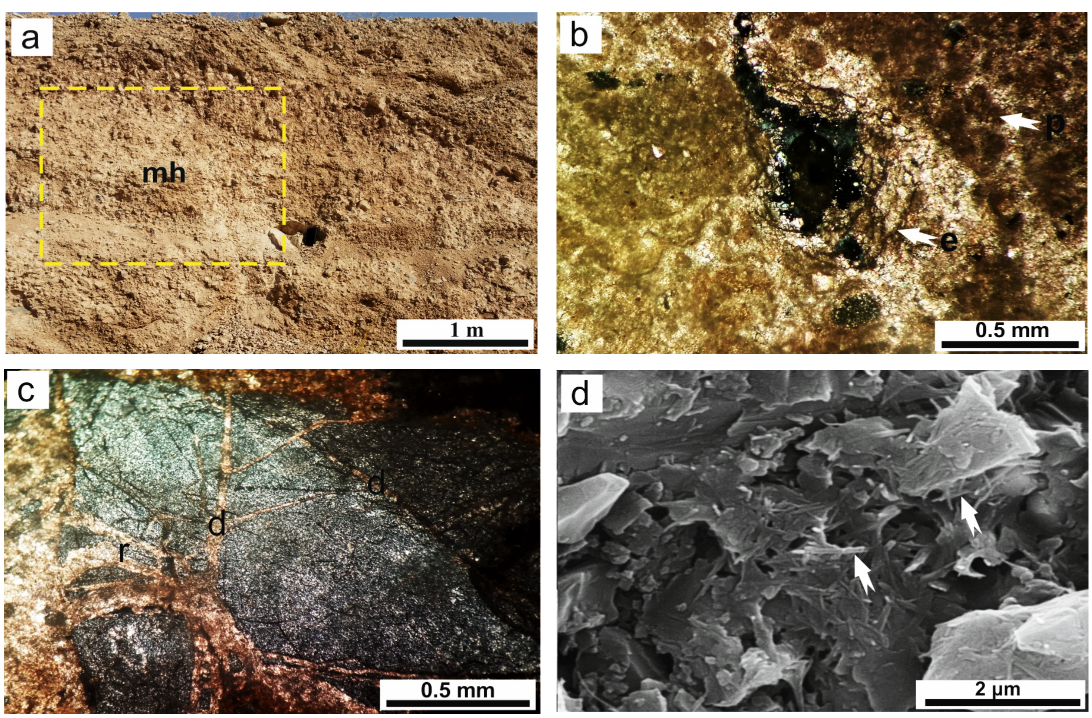

Figure 8. a) Field photograph of the calcrete profile of fan 1 showing massive horizon (mh); b) a root trace and its concentric epidermal sections (e) and diagenetic peloids (p) (XPL); c) Displacement (d), replacement (r), and expansion of host grains (XPL); d) accumulation of host detrital grain and micrite associated with overgrows of fibrous-needle palygorskite (SEM).

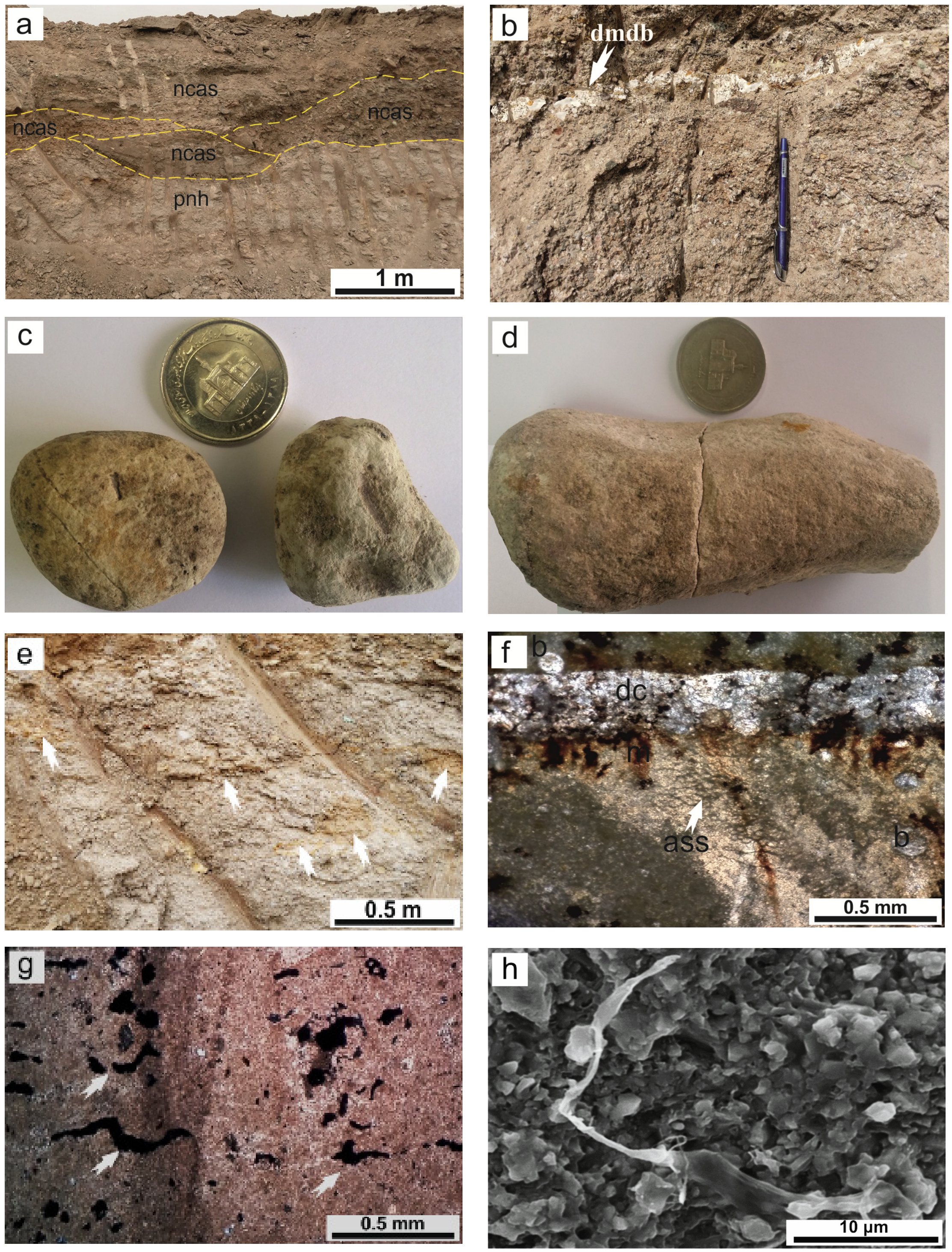

Figure 9. a) Field photograph of the calcrete profile of fan 2: a powdery and nodular horizon (pnh), overlaying by non-calcareous alluvial sediments (ncas); b) diffuse-margin discontinued band (dmdb) of the calcrete profile of fan 2 which mimics the concave-up base plane of the upper channel; c) Disc-shaped and elliptical cream-colored nodules; d) Column-shaped cream colored nodules; the diameter of the coin is 2 cm; e) field photo of mottling (or reddish-brown patches) occur in different parts of calcrete horizon (arrow); f) Desiccation cracks filled with calcite cement (d), bioclasts (b), Mn-oxide mottling along cracks (m), alveolar septal structures (ass), and hair-like roots or filaments (r) in the mature nodule (XPL); g) fenestral porosity (XPL); h) organic filament (SEM); i) Bacterial organisms (SEM); j) pendant various laminae of grain coating consist of exclusively of microsparitic laminea (ms), micritic laminae (m) accompanied with alveolar septal structures (ass), and microsparitic groundmass with abundant clastic grains (msg) (XPL).

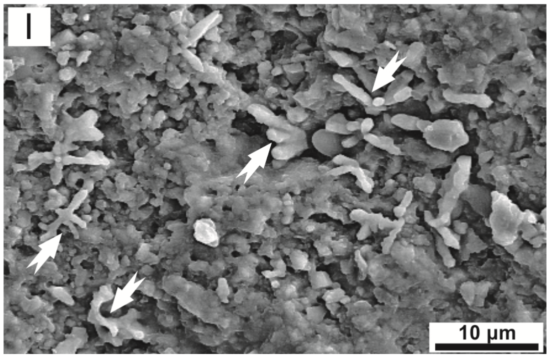

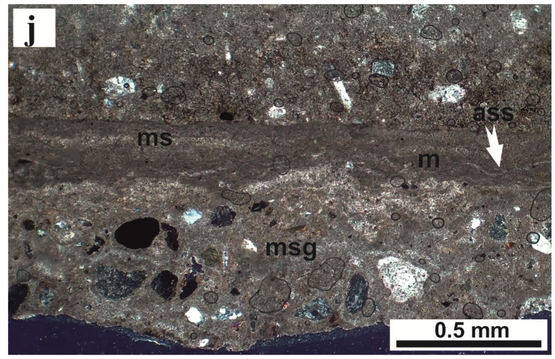

Figure 9. To be continued.

The microfabrics of the discontinuous bands are predominated by alpha microfabrics.

I.3) Type-3 calcrete is found in the distal part of fan 3. The accumulation of secondary carbonate in this profile is in the form of coated grains, patch, and cement. The nucleus of the coated grains is mainly composed of the clasts of the host sediment with various sizes. They have pendent-like coatings and cement. Petrographic study reveals that the coating process has developed various laminae with different colors, thicknesses, and microfabrics such as a) the groundmass consisting exclusively of microsparitic, b) micritic laminae accompanied with root and fungal filaments, and c) thick laminae, formed of microsparitic groundmass with sand- to silt-sized clastic grains (Fig. 9j).

Interpretation

I.1) Based on Machette (1985) calcrete classification, stages V were recognized within the limestone-hosted calcrete profile of fan 1. They are equivalent to the hardpan stage of Esteban and Klappa (1983). The prevalence of coating grains within this profile suggests that the calcretization with the formation of coated grains results from the pedogenic process, which has begun during dry periods in the vadose zone (Wright, 1990; Alonso-Zarza *et al*., 1992). Afterward, the progressive diagenetic alteration of host deposits, such as dissolution and cementation, contributed to blocking of porosity and forming the massive calcrete. This process has occurred during a long-term dry episode with slow or no deposition (Alonso-Zarza *et al*., 1998; Gallala *et al*., 2010). This mature profile has dominantly undergone biogenic, pedogenic, and diagenetic processes. Thus, it can be proposed that this profile has developed under stable climatic, geomorphic, and sedimentation conditions (Reeves, 1976).

I.2) In the lower part of fan 2, the powdery and nodular horizon is present in the distal zone. It is equivalent to the II stages Machette (1985) and Gile (1966), and also the powdery and nodular stages of Esteban and Klappa (1983). The nodules of this horizon are representative of a mature nodule as a result of the pedogenic/biogenic process. Moreover, calcrete diffuse-margin nodules and bands following stratification planes reveal that they have been inorganically precipitated from supersaturated groundwaters migrating along stratification plane or from carbonate-saturated river water (Kadkikar *et al*., 2000; Alonso Zarza & Tanner, 2006), during either carbon dioxide degassing or evaporation (Spotl & Wright, 1992). Aggradation of non-calcrete sediment bodies overlying the calcrete horizon suggests a progressive increase in the sediment supply derived from surrounding highlands through small-scale channels. Aggradation episodes govern the location of the groundwater table, especially in the distal fan areas. In these areas, every new sediment input is followed by a local rising of groundwater level (Alonso-Zarza, 1999), which gives rise to the development of calcrete bands. Therefore, it can be suggested that this horizon has been affected by the pedogenic processes for a long-time, progressive dry, and stable episode, during which the nodules have reached the final maturity. Subsequently, several new sediment supplies have occurred during unstable semi-arid to arid climatic episodes and then the re-calcretization caused by each local rising of the water table during slightly wetter climatic episodes (Alonso-Zarza, 2003; Alonso-Zarza & Wright, 2010).

I.3) The calcrete features in fan 3 are considered as an equivalent to the nodular stage of Esteban and Klappa (1983) and are also equivalent to the Stage I of Gile (1966) and Machette (1985). The diversity of coating laminae of grains in this profile may suggest two main origins: a) biogenic laminae, consisting of roots, cyanobacteria and/or fungal filaments (Beier, 1987; Alonso-Zarza *et al*., 1992) and b) none-biogenic, lacking any organic features, made up of microsparitic groundmass (Hay & Wiggins, 1980). Moreover, the presence of silt and sand sized-detrital grains in the outer most laminae is due to the rolling of the coated grains within the loose host sediments resulting from mechanical force or the activity of the roots (Alonso-Zarza *et al*., 1998). Coated grains are considered to be pedogenic calcretes. The alternating occurrence of thin dark and light laminae followed by a thicker lamina containing detrital grains probably proposes the occurrence of the wet and dry conditions fluctuation followed by a longer dry period.

Petrography and mineralogy of bulk-sediment and clay fraction

Petrographic analysis of the sand fraction of fan 1 sediments show that more than 80% of the samples were derived dominantly from calcareous source rock (Fig. 10 a-b), whereas other fans consist mainly of volcaniclastic, metamorphic, and sedimentary (mainly sandstone and mudstone) rock fragments, alkali feldspar and plagioclase, and minor amounts of quartz and chert (Figs. 10 c-f).

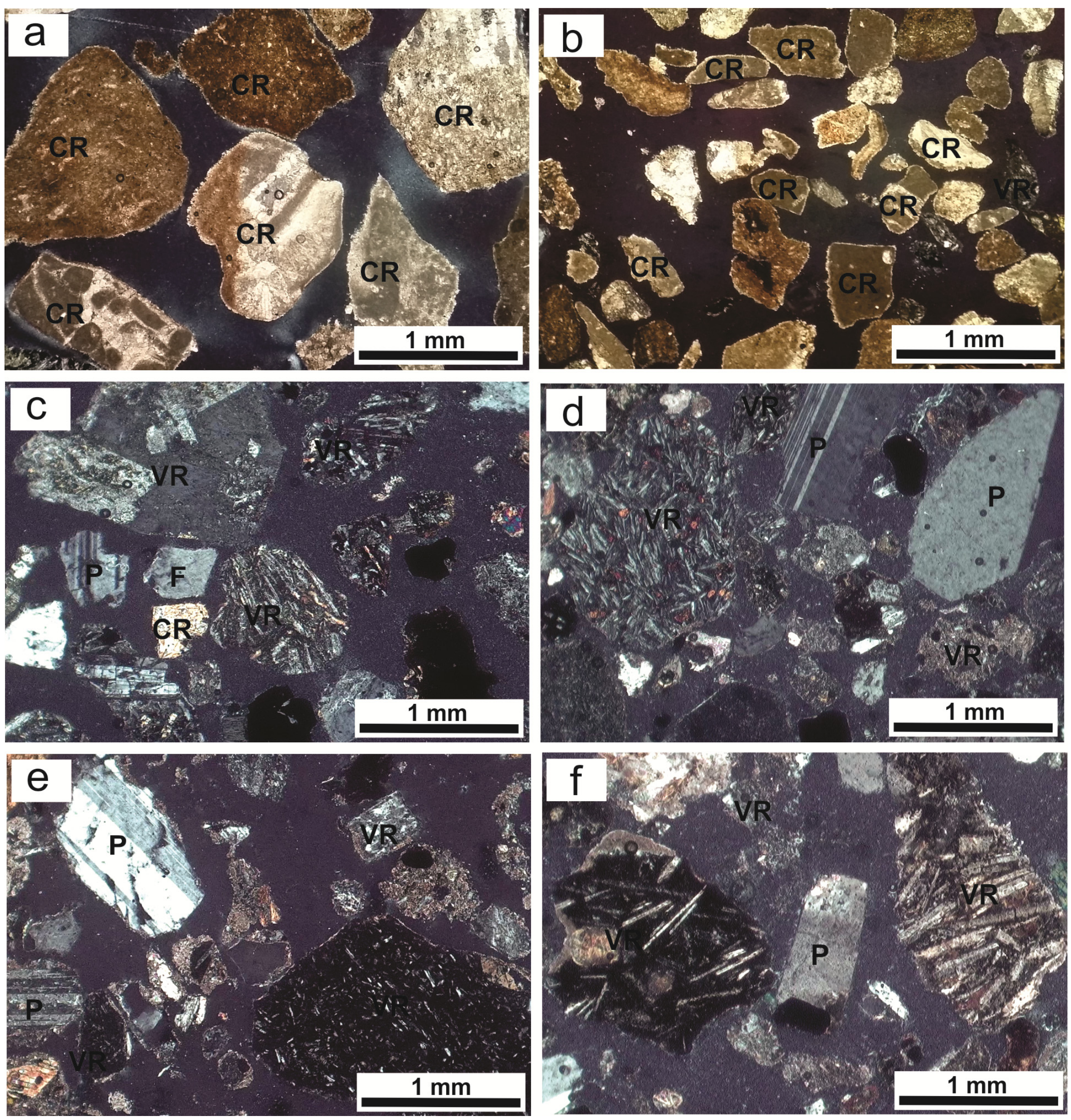

Figure 10. a-b) Microscopic photos of samples of fan 1, showing the abundance of calcareous rock fragments (XPL); c-f) Microscopic photos of samples of fan 2, 3, 4, 5, which also show that the abundance of volcanic rock fragments (XPL). CR: calcareous rock fragment, VR: volcanic rock fragment, P: plagioclase, and F: feldspar.

XRD micrographs of bulk samples represent the predominance of calcite with a high-intensity peak at 29.41 2Θ (3.03Å) (Fig. 11a; Kraemer *et al*., 2005) and the presence of palygorskite, quartz, chlorite, illite, and feldspar. Moreover, diffractograms of clay fractions of calcrete samples of fans 1 and 2 and SEM photomicrographs show that palygorskite is generally high within calcretes (Figs. 11b and c).

The texture of alluvial fan deposits

The debris-flow (Gmm) and lenticular mud-rich facies are common features within all fans. The grain-size data reveal that sediments of fan 1 are relatively finer than other fans (Figs. 12 and 13).

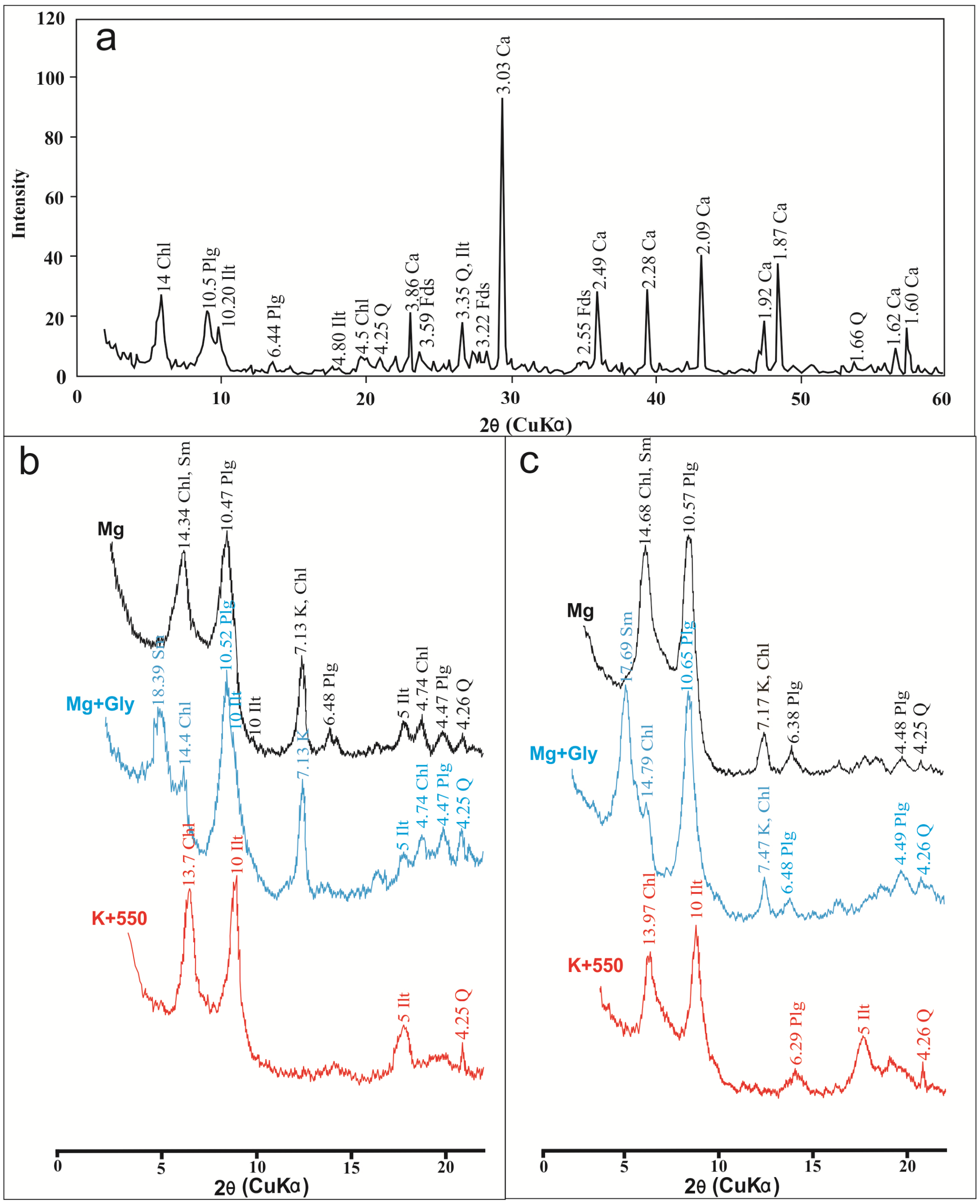

Figure 11. XRD patterns from a) bulk sample of the calcrete profile of fan 1, b) clay fractions of samples from the calcrete profile of fan 1, oriented sample; c) clay fractions of samples from the calcrete profile of fan 2, oriented sample. XRD patterns in black – Mg-saturated air-dried, blue – glycolated, red – heated at 550℃. Abbreviations: plg: palygorskite; Ilt: illite; Sm: Smectite; Chl: chlorite; K: kaolinite; Q: quartz.

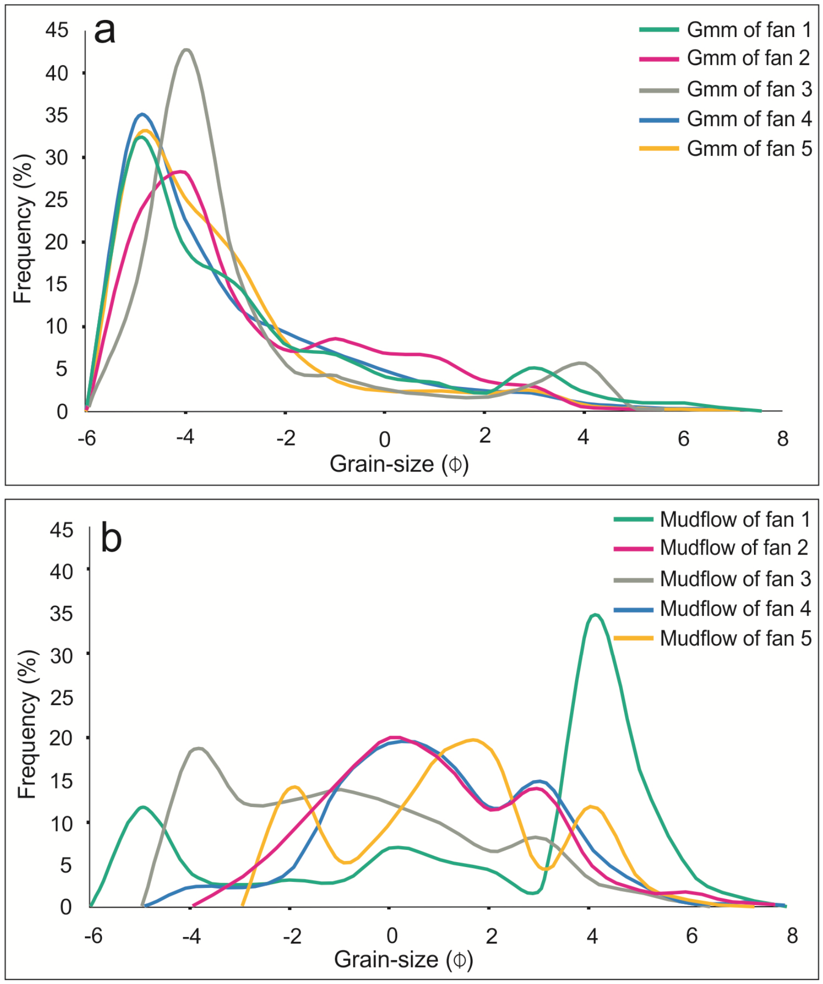

Figure 12. Grain-size distribution of a) the debris flow and b) mudflow facies of the five alluvial fans studied in this research.

The median is approximately 4 mm and the sorting index ranges between 1 and 3, with an average value of 2.1. The matrix of fan 1 shows a slightly better sorting than other fans, with values ranging between 2 and 3 (average of 2.25). The mud content (clay and silt) is considered as a discriminant factor that controls cohesiveness of the sediment-gravity flow (Moscariello *et al*., 2002) and changes over the fans. The clay fraction is generated both by in situ weathering (physical weathering) and by intense biological activity (Moscariello *et al*., 2002). The maximum measured mud content for sediments of fan 1 is 54% (from mudflow), whereas it reaches 9.7% and 5.9 % for fans 2 and 3, respectively. The sediment with the largest grain size (boulder up to block size) typically is derived from massive lithologies of the catchment of fan 3. Blocks and boulders are relatively rare in sediments of the fan 1, where they commonly are scattered within a fine-grained cohesionless matrix.

Discussion

Lithological control on fan processes and sediments

Comparison of sediment-gravity deposits and source area materials shows that the catchment lithology can control the mud content of the resulted deposits and, in turn, control the sedimentary processes on the fan (Moscariello *et al*., 2002). The deposits of fan 1 reveal a rather different texture that may be as a result of the composition of parent material involved and different sedimentary processes. Depending on lithological and mineralogical composition (marly versus pure limestone), the occurrence of heterogeneous intercalations (i.e., interbedded shales), type of cementation, and rock-splitting properties (weathering and tectonic history) of carbonate rocks can produce non-cohesive debris flow (Blair, 1999a).

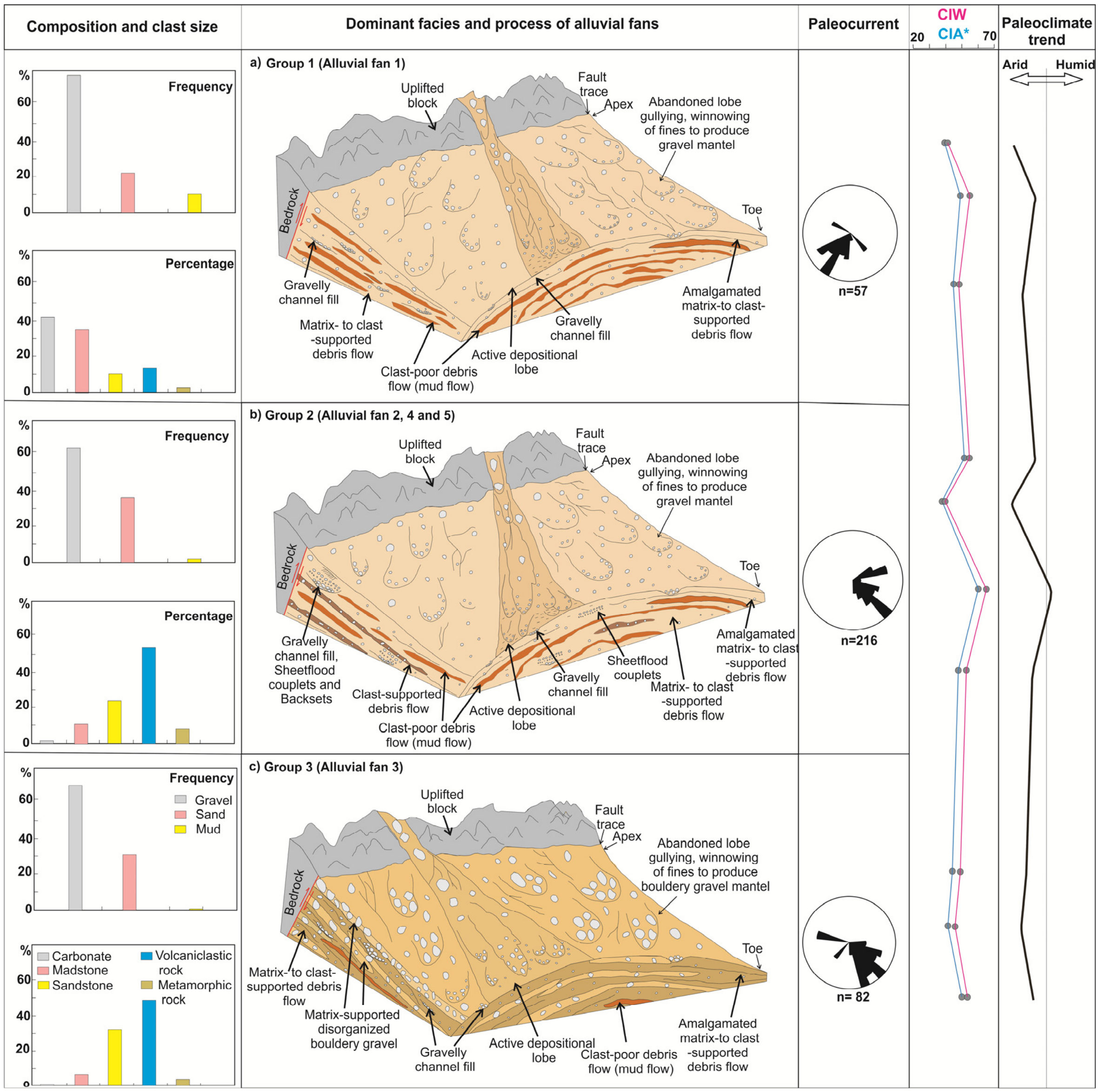

Figure 13. An illustration of grain size and composition, sedimentary facies, chemical weathering, and paleoclimate trend; CIW (Chemical Index of Weathering; Harnois, 1988) and CIA (Chemical Index of Alteration; Nesbitt and Young, 1982).

In the case of deposits generated from calcareous rocks (group 1 lithology), the dominant process will be debris flow, while flash- and sheet-flood processes play a significant role in the sediments of group 2. However, in general, the dominant process of both lithological groups is the non-cohesive debris flow. Furthermore, Ca^{+2} needed for calcretization commonly are generated from calcareous lithologies. That is why the most mature type of calcrete is observed in fan 1 deposits (group 1 lithology).

Paleoclimatic effects on alluvial fan processes

The debris-flow deposits, red-coloration, interbedded mudflow, polygonal mud cracks, and calcretes of the studied areas are indicative of a generally warm and dry climate (Gile *et al*., 1965; Hayward, 1983; Kraus, 1999; Clyde *et al*., 2010), which also exists in other areas of the Qazvin Plain. Subaerial debris flows require abundant clastic debris, a steep slope, and a high discharge for their initiation. Abundant clastic detritus resulting from mechanical weathering during long dry periods are transported by flash floods, with scarce vegetation to inhibit run-off (Miall, 1977). Based on the relative frequency of facies in the study area, three groups (types) of alluvial fans are recognized (Fig. 13). Therefore, based on the frequency (80-95%) of facies A, alluvial fan 1 was formed predominantly by aggregation of poorly sorted, debris-flow lobes, and sheets. In other words, it can be classified as a fan dominated by non-cohesive sediment-gravity flows (type NC-4) of Blair and MacPherson (2009). Such fans are special cases arising from non-cohesive colluvium, which is formed by clay-poor colluvium during catastrophic discharge. The minor volume of runoff-related lenticular gravely units (~10-15%) reveals that the contribution of floods to primary aggradation of the fan is insignificant and only locally redistribute sediment on the fan surface (Fig. 2d). Interbedded red colored mudflows suggest that aggradation process of the alluvial fan was episodic rather than a constant process of delivery. An indication of episodic deposition and laterally unconfined nature of flows, suggestive of debris flow deposition (Blair & McPherson, 2009; Mather, 2016), is abundantly observed in other fans (~ 60-70%). However, the contribution of deposits resulting from flash and sheetfloods in their deposits is about 30-40%.

The non-cohesive debris flows originate from the catchment with low mud (especially clay) content. Granulometric results revealed that mud volume of all fans (excluding mudflows) is low (<5%). This low mud content is probably due to the fact that the clay and the silt-sized fraction is a minor product in the arid climate because they form either by hydrolysis of feldspar and accessory minerals or through tight tectonic shearing (Blair, 1999c, 2003). However, such reactions are slow in arid settings because mud production requires long periods of high-moderate humidity (Blair & McPherson, 2009). These fans can be correlated with interbedded red colored mudflow (Table 1) indicating an extremely dry climate (Yan *et al*., 2007). In addition, the aridification during the Quaternary can be inferred based on calcrete features (Hasegawa *et al*., 2009), especially the occurrence of palygorskite as a particular clay mineral of calcretes (Figs. 8d and 11) (AlShuaibi & Khalaf, 2011; Zucca *et al*., 2017).

Moreover, paleoclimate and paleo-weathering can be inferred from the elemental geochemistry of sedimentary rocks. Therefore, the low degree of weathering is the result of the arid climate, whereas the high degree of weathering is related to a warm and humid climate (Nesbitt and Young, 1982). Generally, we use the Chemical Index of Alteration (CIA) and the Chemical Index of Weathering (CIW) to assess chemical weathering. Overall, the CIA and CIW values of the samples support the relatively poor degree of chemical weathering. However, the highest values of CIA and CIW is related to the sample of fan 4, suggesting that this fan probably experienced relatively more intense chemical weathering (Fig. 13).

Tectonic controls on the development of the fans and depositional processes

Clast compositions and the analysis of paleocurrent directions based on the preferred orientations of the elongate clasts support that the sediments of all the studied fans were mainly transported in an S-SE direction. Therefore, the tectonic uplift resulting from faulting has controlled the accumulation loci of the fans. In addition, the most striking impact of tectonic on depositional processes can be seen in fan 3. The marked differences of fan 3 in facies (facies B) and clast size, from apex to toe, are possibly due to the reactivation of the fan head faults induced by the catastrophic collapse of the local source rocks. The clasts of this facies are obviously related to local lithology and delivered from physical weathering and brittle disintegration associated with fault movement. In addition, the wide range of sediments from clay to boulders probably facilitated transformation into debris-flows (Blair, 1999b; Blair & McPherson, 2009). In contrast, the relatively stable tectonic background and arid to semi-arid climate (Reeves, 1983; Wright & Tucker, 1991) may be considered as the main reasons for the development of calcrete in some horizons of the studied profiles.

Conclusions

The study of 5 modern alluvial fans throughout the Qazvin Plain led to the diagnosis of three different groups of fans in facies. Eight facies were identified and generally interpreted as the following depositional processes: 1) non-cohesive debris flows, 2) sub-aerial mud-rich debris flows, 3) channelized non-cohesive debris flows, 4) hyperconcentrated flows, and 5) sheetfloods. More than 85% of the deposits were formed by the first process. The other dominant processes in those fans are sourced from volcanic rocks (fans 2, 3, 4, and 5).

The arid to semi-arid climate was likely to have favored debris flows on fans of the Qazvin Plain. Such climatic conditions are expressed by the development of calcrete. Climatic aridification led to a decrease in mud (especially clay) content and thus increased the occurrence of non-cohesive debris-flows on the alluvial fans. Therefore, the differences in the tectonic activities, climate, and bedrock types are considered as a controlling factor of the sedimentary processes.

Acknowledgments

We would like to express our special thanks to: 1- The head of the Abyek Cement Factory for assistance in field data collection 2- The President and the Research Dean of Bu-Ali Sina University for financial support.

References

Alenander, J., Fielding, C., 1997. Gravel antidunes in the tropical Burdekin River, Queensland, Australia. Sedimentology, 44: 327–337.

Allen, M.B., Ghassemi, M.R., Shahrabi, M., Qorashi, M., 2003. Accommodation of Late Cenozoic oblique shortening in the Alborz range, northern Iran. Journal of Structural Geology, 25: 659–672. In Persian.

Alonso-Zarza, A.M., 1999. Initial stages of laminar calcrete formation by roots: examples from the Neogene of central Spain. Sedimentary Geology, 126: 177–191.

Alonso-Zarza, A.M., 2003. Palaeoenvironmental significance of palustrine carbonates and calcretes in the geological record. Earth Science Review, 60: 261 –298.

Alonso-Zarza, A.M., Silva, P.G., Goy, J.L., Zazo, C., 1998. Fan-surface dynamics and biogenic calcrete development: Interactions during ultimate phases of fan evolution in the semiarid SE Spain (Murciaz). Geomorphology, 24: 147–167.

Alonso-Zarza, A.M., Tanner, L.H., 2006. Paleoenvironmental record, applications of calcretes, plaustrine carbonates. Geological Society of America Bulletin, 416: 416, 239.

Alonso-Zarza, A.M., Wright, V.P., 2010. Calcretes. In: Alonso-Zarza, A.M., Tanner, L.H. (Eds.), Carbonates in Continental Settings: Facies, Environments and Processes. Developments in Sedimentology. Elsevier, Amsterdam, 61: 225–268.

Alonso-Zarza, M.A., Calvo, J.P., Garcıa Del Cura, M.A., 1992. Palustrine sedimentation and associated features–grainification and pseudo-microkarst–in the Middle Miocene (intermediate unit) of the Madrid Basin Spain. Sedimentary Geology, 76: 43–61.

AlShuaibi, A.A., Khalaf, F.I., 2011. Development and lithogenesis of the palustrine and calcrete deposits of the Dibdibba Alluvial Fan, Kuwait. Journal of Asian Earth Science, 42: 423–439.

Amajor, L.C., 1986. Alluvial Fan facies in the Miocene-pliocene coastal plain sands, Niger Delta, Nigeria. Sedimentary Geology, 49: 1-20.

Annells, R.N., Arthurton, R.S., Bazley, R.A., Davies, R.G., 1975. Explanatory text of the Qazvin and Rasht quadrangles map. 1:250.000. Geological Survey of Iran. Geological Quadrangles Nos. E3-E4. In Persian.

Araya, T., Masuda, F., 2001. Sedimentary structures of antidunes: An overview. Journal of the Sedimentological Society of Japan, 53: 1–15.

Barwis, J.H., Hayes, M., 1985. Antidunes on modern and ancient washover fans. Journal of Sedimentary Petrology, 55: 907–916.

Beier, J.A., 1985. Diagenesis of Quaternary Bahamian beach rock: petrographic and isotopice vidence. Journal of Sedimentary Petrology, 55: 755–761.

Berberian, M., Qorashi, M., Arzhang-ravesh, B., Mohajer-Ashjai, A., 1993. Recent tectonics, seismotectonics and earthquake-fault hazard investigation in the Greater Qazvin region:contribution to the seismotectonics of Iran, part VI. Geology Survey of Iran, 197 pp.

Blair, T.C., McPherson, J.G., 1998. Recent debris-flow processes and resultant form and facies of the dolomite alluvial fan, Owens valley, California. Journal of Sedimentary Research 68/5, s. 800 – 818.

Blair, T.C., 1999 a. Sedimentary processes and facies of the waterlaid Anvil Spring Canyon alluvial fan, Death Valley, California. Sedimentology, 46: 913–940.

Blair, T.C., 1999 b. Cause of dominance by sheetflood vs. debris-flow processes on two adjoining alluvial fans, Death Valley, California. Sedimentology, 46: 1015–1028

Blair, T.C., 1999 c. Form, facies, and depositional history of the North Long John rock avalanche, Owens Valley, California. Canadian Journal of Earth Sciences, 36: 855–870.

Blair, T.C., 2001. Outburst flood sedimentation on the proglacial Tittle canyon alluvial fan, Owens Valley, California, U.S.A. Journal of Sedimentary Research, 71: 658–680.

Blair, T.C., 2003. Features and origin of the giant Cucomungo Canyon alluvial fan, Eureka Valley, California. In: Chan MA, Archer AW (eds.) Extreme depositional environments: Mega end members in geologic time. Geological Society of America Special Paper, 370: 105–126.

Blair, T.C., McPherson, J. G., 1994. Alluvial fans and their natural distinction from rivers based on morphology, hydraulic processes, sedimentary processes and facies assemblages. Journal of Sedimentary Research, 64 (3): 450-489.

Blair, T.C., McPherson, J.G., 1998. Recent debris flow processes and resultant form and facies of the Dolomite alluvial fan, Owens Valley, California. Journal of Sedimentary Research, 68: 800– 818.

Blair, T.C., McPherson, J.G., 2009. Processes and forms of alluvial fans. Chapter 14, In: Parsons, A.J., Abrahams, A.D. (Eds.). Geomorphology and Desert Environments, 413–467.

Bluck, B.J., 1980. Structure, generation and preservation of upward fining, braided stream cycles in the Old Red Sandstone of Scot- land. Transactions of the Royal Society of Edinburgh, 71: 29–46.

Blum, M.D., Tornqvist, T.E., 2000. Fluvial responses to climate and sea level change: A review and look forward. Sedimentology, 47: 2–48.

Bose, P.K., Eriksson, P.G., Sarkar, S., Wright, P., Samanta, P., Mukhopadhyay, S., Mandal, S., Banerjee, S., Altermann, W., 2012. Sedimentation patterns during the Precambrian: Precambrian: a unique record? Marine and Petroleum Geology, 33: 34–68.

Bull, W.B., 1972. Recognition of alluvial fan deposits in the stratigraphic record. In: J.K. Rigby and W.K. Hamblin (Editors), Recognition of Ancient Sedimentary Environments. Society of Economic Paleontologists and Mineralogists, 16: 63–83.

Chakraborty, P.P., Paul, P., 2013. Depositional character of a dry-climate alluvial fan system from Palaeoproterozoic rift setting using facies architecture and palaeohydraulics: Example from the Par Formation, Gwalior Group, central India. Journal of Asian Earth Sciences, 91: 298-315.

Chen, L., Steel, R.J., Guo, F., Olariu, C., Gong, C., 2016. Alluvial fan facies of the Yongchong Basin: Implications for tectonic and paleoclimatic changes during Late Cretaceous in SE China, Journal of Asian Earth Sciences, 134: 37–54.

Clyde, W.C., Ting, S.Y., Snell, K.E., Bowen, G.J., Tong, Y.S., Koch, P.L., Li, Q., Wang, Y.Q., 2010. New Paleomagnetic and Stable-Isotope Results from the Nanxiong Basin, China: Implications for the K/T Boundary and the Timing of Paleocene Mammalian Turnover. Journal of Geology, 118: 131–143.

Copley, A., Jackson, J., 2006. Active tectonics of the Turkish-Iranian Plateau. Tectonics. 25 (TC6006), 1–19.

De Haas, T., Ventra, D., Carbonneau, P.E., Kleinhans, M.G., 2014. Debris-flow dominance of alluvial fans masked by runoff reworking and weathering. Geomorphology, 217: 165–181.

Esteban, M., Klappa, C.F., 1983. Subaerial exposure. In: Scholle, P.A., Bebout, D.G., Moore, C.H. (Eds.), Carbonate Depositional Environments. Memoir? American Association of Petroleum Geologists Convention, 33: 1–54.

Frostick, L.E., Reid, I., 1989. Climatic versus tectonic controls of fan sequences: lessons from the Dead Sea, Israel. Journal of the Geological Society of London, 146: 527–538.

Gallala, W., Essghaier Gaied, M., Montacer, M., 2010. Pleistocene calcretes from eastern Tunisia: The stratigraphy, the microstructure and the environmental significance. Journal of African Earth Sciences, 58:445–456.

Galloway, W.E., 1996. Terrigenous Clastic Depositional Systems. Springer-Verlag Berlin Heidelberg.

Gawthorpe, R.L., Leeder, M.R., 2000. Tectono-sedimentary evolution of active extensional basins. Basin Research, 12: 195–218.

Ghinassi, M., Ielpi, A., 2016. Morphodynamics and facies architecture of stream flow-dominated, sand-rich alluvial fans, Pleistocene Upper Valdarno Basin, Italy. In: Ventra, D. & Clarke, L.E. (eds) Geology and Geomorphology of Alluvial and Fluvial Fans: Terrestrial and Planetary Perspectives. Geological Society, London, Special Publications, 440. First published online February 10, 2016, https://doi.org/10.1144/ SP440.1.

Gile, L.H., Peterson, F.F. Grossman, R.B., 1965. The K horizon: a master horizon of carbonate accumulation. Journal of Soil Science, 97: 74–82.

Gile, L.H., Peterson, F.F., Grossman, R.B., 1966. Morphological and genetic sequences of carbonate carbonate accumulation in desert soils. Journal of Soil Science, 101: 347–360.

Harms, J.C., Fahnestock, R.K., 1965. Stratification, bed forms, and flow phenomena (with an example from the Rio Grande), in Middleton, G.V., ed., Primary Sedimentary Structures and Their Hydrodynamic Interpretation: Society for Economic Paleontologists and Mineralogists (SEPM) Special Publication, 12: 84–115.

Harnois, L., 1988. The CIW index: a new chemical index of weathering. Sedimentary Geology, 55: 319–322.

Harvey, A.M., 2012. The coupling status of alluvial fans and debris cones: a review and synthesis. Earth Surface Processes and Landforms, 37: 64–76.

Harvey, A.M., Mather, A.E., Stokes, M., 2005. Alluvial fans: geomorphology, sedimentology, dynamics – introduction. A review of alluvial-fan research. In: Harvey, A.M., Mather, A.E., Stokes, M. (Eds.), Alluvial fans: geomorphology, sedimentology, dynamics. Geological Society Special Publication, 251: 1–8.

Hasegawa, H., Tada, R., Ichinnorov, N., Minjin, C., 2009. Lithostratigraphy and depositional environments of the Upper Cretaceous Djadokhta Formation, Ulan Nuur Basin, southern Mongolia, and its paleoclimatic implication. Journal of Asian Earth Sciences, 35: 13–26.

Hay, R.L., Wiggins, B., 1980. Pellets, ooids, sepiolite and silica in three calcretes of the southwestern United States. Sedimentology, 27: 559–576.

Hayward, A.B. 1983. Coastal alluvial fans and associated marine facies in the Miocene of S.W. Turkey. International Association of Sedimentologists, 6: 323–336.
Hwang, G., Gihm, Y.S., Kim, M.C., 2016. Supercritical sheetflood deposits on the volcaniclastic alluvial fan: the Cretaceous upper Daeri Member, Wido Island, Korea. Geophysical Research Abstracts, 18: 3612–1.
Kastic, B., Bech, A., Antiger, T., 2005. 3-D sedimentary architecture of a Quaternary gravel delta (Sw-Germany): Implication for hydrostratigraphy sedimentary Geology. Sedimentary Geology, 181(3-4): 147–171.
Khadkikar, A.S., Chamyal, L.S., Ramesh, R., 2000. The character and genesis of calcrete in Late Quaternary alluvial deposits, Gujarat, western India, and its bearing on the interpretation of ancient climates. palaeogeogr palaeoclimatol palaeoecol, 162: 239–261.
Kleinhans, M.G. van Rijn, L.C., 2002. Stochastic prediction of sediment transport in sand-gravel Bed Rivers. Journal of Hydraulic Engineering, Special Issue on Stochastic Sediment Transport and Hydraulics, 128(4): 412–425.
Kraimer, R.A., Monger, H.C., Steiner, R.L., 2005. Mineralogical distinction of carbonates in desert soils. Soil Science Society of America Journal, 69: 1773–1781.
Koltermann, C.E., Gorelick, S.M., 1992. Paleoclimatic signature in terrestrial flooddeposits. Science, 256: 1775–1782.
Kraus, M.J., 1999. Paleosols in clastic sedimentary rocks: their geologic applications. Earth-Science Review, 47: 41–70.
Lindsey, D.A., Langer, W.H., Knepper, D.H., 2005. Stratigraphy, lithology, and sedimentary features of Quaternary alluvial deposits of the South Platte River and some of its tributaries east of the Front Range, Colorado: U.S. Geological Survey Professional Paper, 1705: 70 pp.
Machette, M.N., 1985. Calcic soils of the southwestern United States. In: Weide, D.I., Faber, M.L. (Eds.), Soils and Quaternary Geology of the Southwestern United States. Geological Society of America Special Paper, 203: 1–21.
Martini, I.P., 1977. Gravelly flood deposits of Irvine Creek, Ontario, Canada. Sedimentology, 24: 603-622.
Masuda, F., Yokokawa, M., Sakamoto, T., 1993. HCS mimics in Pleistocene, tidal deposits of the Shimosa Group and flood deposits of the Osaka Group, Japan. Journal of the Sedimentological Society of Japan, 39: 27–34.
Mather, A.E., Stokes, M., Whitfiel, E., 2016. River terraces and alluvial fans: The case for an integrated Quaternary fluvial archive, Quaternary Science Reviews, 166: 74–90.
Meteorological Organization of Iran, 2011. www.irimo.ir/eng.
Miall, A.D., 1977. A review of the braided river depositional environment. Earth Science Reviews, 13: 1–62.
Miall, A.D., 2006. The Geology of Fluvial Deposits: Sedimentary Facies, Basin Analysis, and Petroleum Geology, Springer, 582 pp.
Middleton, G., 1965. Antidune cross-bedding in a large flume. Journal of Sedimentary Petrology, 35: 922-927.
Moscariello, A., 2017. Alluvial fans and fluvial fans at the margins of continental sedimentary basins: geomorphic and sedimentological distinction for geo-energy exploration and development. Geological Society, London, Special Publications, 440, https://doi.org/10.1144/SP440.11.
Moscariello, A., Marchi, L., Maraga, F., Mortara, G., 2002. Alluvial fans in the Italian Alps: sedimentary facies and processes. International Association of Sedimentologists Special Publication, 32: 141–66.
Mutti, E., Davoli, G., Tinterri, R., Zavala, C., 1996. The importance of fluvio-deltaic systems dominated by catastrophic flooding in tectonically active basins. Science Geologiques Memoires, 48: 233–291.
Nemec, W., Steel, R.J., 1984. Alluvial and coastal conglomerates: Their significant features and some comments on gravely mass-flow deposits. In: Koster, E.H., Steel, R.J. (Eds.), Sedimentology of Gravels and Conglomerates: Canadian Society of Petroleum Geologists, Geologists, 10: 1–31.
Nesbitt, H.W., Young, G.M., 1982. Early Proterozoic climates and plate motions inferred from major element chemistry of lutites. Nature, 299: 715–717.
Nichols, G., Thompson, B., 2005. Bedrock lithology control on contemporaneous alluvial fan facies, Oligo-Miocene, southern Pyrenees, Spain. Sedimentology, 52: 571–585.
Parker, G., Sutherland, A.J., 1990. Fluvial armor. Journal of Hydraulic Research, 28(5): 529–544.
Postma, G., 1984. Slumps and their deposits in fan delta front and slope. Geology, 12: 27–30.
Reeves, C.C., 1983. Pliocene channel calcrete and suspenparallel drainage in West Texas and New Mexico. In: Wilson, R.C.L. (Eds.), Residual Deposits: Surface Related Weathering Processes and Materials. Geological Society of London Special Publication. Geological Society of London, 11: 179–183.
Rieben, E.H., 1966. Geological observations on alluvial depositions in northern Iran. Geological Survey of Iran, 39 pp.
Rodine, J.D., Johnson, A.M., 1976. The ability of debris heavily freighted with coarse clastic material to flow on gentle slopes. Sedimentology, 23: 213–234.
Rust, B.R., Gibling, M.R., 1990. Three-dimensional antidunes as HCS mimics in a fluvial sandstone: the Pennsylvanian South Bar Formation near Sydney, Nova Scotia. Journal Sedimentary Research, 60: 540–548.
Sanchez-Nunez, J.M., Maclas, J.L., Zamorano, J.J., Novelo, D., Mendoza, M.E., Torres-Hernandez, J.R., 2014. Geomorphology, internal structure and evolution of alluvial fans at Motozintla, Chiapas, Mexico. Geomorphology, doi: 1016/j. geomorph. 2014.10.003. pp 43.

Sarkar, S., Bose, P.K., Samanta, P., Sengupta, P., Eriksson, P.G., 2008. Microbial mat mediated structures in the Ediacaran Sonia Sandstone, Rajasthan, India, and their implications for proterozoic sedimentation. Precambrian Research, 162: 226–248.

Saula, E., Mato, E., Puigdefabregas, C., 2002. Catastrophic debrisflow deposits from an inferred landslide-dam failure, the Eocene Berga Formation, eastern Pyrenees, Spain. In: Baker, V., Martini, I.P., Garzon, G. (Eds.), Floods and Megafloods Processes and Deposits. International Association of Sedimentologists, Oxford, Special Publication, 32: 195–209.

Schultz, A.W., 1984. Subaerial debris flow deposition in the Upper Paleozoic Cutler Formation, western Colorado: Journal of Sedimentary Petrology, 54: 759–772.

Schumm, S.A., 1977. The fluvial system. John Wiley & Sons, Inc., New York, N.Y.

Slootman, A., Simpson, G., Castelltort, E., De Boer. P.L., 2018. Geological record of marine tsunami-backwash: the role of the hydraulic jump. The journal of the International Association of Sedimentologists, doi: 10.1002/dep2.38.

Sohn, Y.K., Rhee, C.W., Kim, B.C., 1999. Debris flow and hyperconcentrated flood-flow deposits in an alluvial fan, northwestern part of the Cretaceous Yongdong Basin, Central Korea. Journal of Geology, 107: 111–132.

Spotl, C., Wright, V.P., 1992. Groundwater dolocretes from the Upper Triassic of the Paris Basin, France: a case study of an arid, continental diagenetic facies. Sedimentology, 39: 1119–1136.

Turkmen, A., Aksoy, E., Taogin, C.K., 2007. Alluvial and lacustrine facies in an extensional basin: The Miocene of Malatya basin, eastern Turkey. Journal of Asian Earth Sciences, 30: 181–198.

Walker, R.G., 1975. Conglomerate: Sedimentary structures and facies models. In: J.C. Harms, J.B. Southard, D.R. Spearing and R.G. Walker (Editors), Depositional Environments as Interpreted from Primary Sedimentary Structures and Stratification Sequences. Society of Economic Paleontologists and Mineralogists, 2: 133–158.

Walker, T.R., 1967. Formation of red beds in modern and ancient deserts. Geological Society of America Bulletin, 78: 917–920.

Went, D.J., 2005. Pre-vegetation alluvial fan facies and pro- cesses: an example from the Cambro-Ordovician Rozel Conglomerate Formation, Jersey, Channel Islands. Sedimentology, 52: 693–713.

Wright, V.P., 1990. Syngenetic formation of grainstones and pisolites from fenestral carbonates in peritidal settings: discussion. Journal of Sedimentary Petrology, 60: 309–310.

Wright, V.P., Tucker, M.E., 1991. Calcretes. An introduction. In: Wright, V.P., Tucker, M.E. (Eds.), Calcretes. IAS Reprint Series. Blackwell, Oxford, 2: 1–22.

Yan, Y., Xia, B., Lin, G., Cui, X., Hu, X., Yan, P., Zhang, F., 2007. Geochemistry of the sedimentary rocks from the Nanxiong Basin, South China and implications for provenance, paleoenvironment and paleoclimate at the K/T boundary. Sedimentary Geology, 197: 127–140.

Zucca, C., Previtali, F., Madrau, S., Kadir, S., Eren, M., Akca, E., Kapur, S., 2017. Microstructure and palygorskite neoformation in pedogenic calcretes of central Morocco. Catena, 168: 141–152.